

# KEYLINK: towards a more integrative soil representation for inclusion in ecosystem scale models. II. Model description, implementation and testing

Omar Flores<sup>Corresp., Equal first author, 1, 2</sup>, Gaby Deckmyn<sup>Equal first author, 2</sup>, Jorge Curiel Yuste<sup>3, 4</sup>, Mathieu Javaux<sup>5, 6</sup>, Alexei Uvarov<sup>7</sup>, Sietse van der Linde<sup>8</sup>, Bruno De Vos<sup>9</sup>, Harry Vereecken<sup>6</sup>, Juan Jiménez<sup>10</sup>, Olga Vinduskova<sup>2</sup>, Andrea Schnepf<sup>6</sup>

<sup>1</sup> Biogeography and Global Change, National Museum of Natural Sciences, Consejo Superior de Investigaciones Científicas, Madrid, Spain

<sup>2</sup> PLECO, Department of Biology, Universiteit Antwerpen, Antwerp, Belgium

<sup>3</sup> BC3 - Basque Centre for Climate Change, Leioa, Spain

<sup>4</sup> IKERBASQUE - Basque Foundation for Science, Bilbao, Spain

<sup>5</sup> Earth and Life Institute, Université Catholique de Louvain, Louvain-la-Neuve, Belgium

<sup>6</sup> Agrosphere Institute (IBG-3), Forschungszentrum Jülich GmbH, Jülich, Germany

<sup>7</sup> Laboratory of Soil Zoology, A.N. Severtsov Institute of Ecology and Evolution, Russian Academy of Sciences, Moscow, Russia

<sup>8</sup> Forest Research, Farnham, United Kingdom

<sup>9</sup> Department of Environment and Climate, Research Institute for Nature and Forest, Brussels, Belgium

<sup>10</sup> Instituto Pirenaico de Ecología, Consejo Superior de Investigaciones Científicas, Jaca, Spain

Corresponding Author: Omar Flores

Email address: omar.flores@uantwerpen.be

New knowledge on soil structure highlights its importance for hydrology and soil organic matter (SOM) stabilization, which however remains neglected in many wide used models. We present here a new model, KEYLINK, in which soil structure is integrated with the existing concepts on SOM pools, and elements from food web models, i.e. those from direct trophic interactions among soil organisms. KEYLINK is, therefore, an attempt to integrate soil functional diversity and food webs in predictions of soil carbon (C) and soil water balances. We present a selection of equations that can be used for most models as well as basic parameter intervals for, e.g., key pools, functional groups' biomasses and growth rates. Parameter distributions can be determined with Bayesian calibration, and here an example is presented for food web growth rate parameters for a pine forest in Belgium. We show how these added equations can improve the functioning of the model in describing known phenomena. For this, five test cases are given as simulation examples: changing the input litter quality (recalcitrance and carbon to nitrogen ratio), excluding predators, increasing pH and changing initial soil porosity. These results overall show how KEYLINK is able to simulate the known effects of these parameters and can simulate the linked effects of biopore formation, hydrology and aggregation on soil functioning. Furthermore, the results show an important trophic cascade effect of predation on the complete C cycle with repercussions on the soil structure as ecosystem engineers are

predated, and on SOM turnover when predation on fungivore and bacterivore populations are reduced. In summary, KEYLINK shows how soil functional diversity and trophic organization and their role in C and water cycling in soils should be considered in order to improve our predictions on C sequestration and C emissions from soils.

1 **KEYLINK: towards a more integrative soil representation for**  
2 **inclusion in ecosystem scale models. II. Model description,**  
3 **implementation and testing.**

4

5 **Omar Flores**<sup>Corresp., Equal first author, 1, 2\*</sup>, **Gaby Deckmyn**<sup>Equal first author, 2</sup>, **Jorge Curiel Yuste**<sup>3, 4</sup>,  
6 **Mathieu Javaux**<sup>5,6</sup>, **Alexei Uvarov**<sup>7</sup>, **Sietse van der Linde**<sup>8</sup>, **Bruno De Vos**<sup>9</sup>, **Harry**  
7 **Vereecken**<sup>6</sup>, **Juan Jiménez**<sup>10</sup>, **Olga Vinduskova**<sup>2</sup>, **Andrea Schnepf**<sup>6</sup>

8

9 <sup>1</sup>Department of Biogeography and Global Change, National Museum of Natural Sciences -  
10 Spanish National Research Council (MNCN-CSIC), Madrid, Spain

11 <sup>2</sup>Centre of Excellence PLECO, Department of Biology, Universiteit Antwerpen, Antwerp,  
12 Belgium

13 <sup>3</sup>BC3-Basque Centre for Climate Change, Leioa, Spain

14 <sup>4</sup>IKERBASQUE - Basque Foundation for Science, Bilbao, Spain

15 <sup>5</sup>Earth and Life Institute, Université Catholique de Louvain, Louvain-la-Neuve, Belgium

16 <sup>6</sup>Agrosphere Institute (IBG-3), Forschungszentrum Jülich GmbH, Jülich, Germany

17 <sup>7</sup>Laboratory of Soil Zoology, A.N. Severtsov Institute of Ecology and Evolution, Russian  
18 Academy of Sciences, Moscow, Russia

19 <sup>8</sup>Forest Research, Farnham, United Kingdom

20 <sup>9</sup>Department of Environment and Climate, Research Institute for Nature and Forest, Brussels,  
21 Belgium

22 <sup>10</sup>ARAID, Pyrenean Institute of Ecology - Spanish National Research Council (IPE-CSIC), Jaca,  
23 Spain

24

25 **Corresponding Author:**

26 Omar Flores<sup>1,2</sup>

27 Universiteitsplein 1, Wilrijk, 2610, Belgium

28 Email address: dr.flores.omar@gmail.com

29

30 **Abstract**

31 New knowledge on soil structure highlights its importance for hydrology and soil organic matter  
32 (SOM) stabilization, which however remains neglected in many wide used models. We present  
33 here a new model, KEYLINK, in which soil structure is integrated with the existing concepts on

34 SOM pools, and elements from food web models, i.e. those from direct trophic interactions  
35 among soil organisms. KEYLINK is, therefore, an attempt to integrate soil functional diversity  
36 and food webs in predictions of soil carbon (C) and soil water balances. We present a selection  
37 of equations that can be used for most models as well as basic parameter intervals for, e.g., key  
38 pools, functional groups' biomasses and growth rates. Parameter distributions can be determined  
39 with Bayesian calibration, and here an example is presented for food web growth rate parameters  
40 for a pine forest in Belgium. We show how these added equations can improve the functioning of  
41 the model in describing known phenomena. For this, five test cases are given as simulation  
42 examples: changing the input litter quality (recalcitrance and carbon to nitrogen ratio), excluding  
43 predators, increasing pH and changing initial soil porosity. These results overall show how  
44 KEYLINK is able to simulate the known effects of these parameters and can simulate the linked  
45 effects of biopore formation, hydrology and aggregation on soil functioning. Furthermore, the  
46 results show an important trophic cascade effect of predation on the complete C cycle with  
47 repercussions on the soil structure as ecosystem engineers are predated, and on SOM turnover  
48 when predation on fungivore and bacterivore populations are reduced. In summary, KEYLINK  
49 shows how soil functional diversity and trophic organization and their role in C and water  
50 cycling in soils should be considered in order to improve our predictions on C sequestration and  
51 C emissions from soils.

52

## 53 **Introduction**

54 Soil models used in ecosystem-scale modelling need to be relatively simple and fast at  
55 performing calculations. Nonetheless, carbon (C) and nutrient turnover and hydrology are  
56 extremely important for determining ecosystem productivity and C sequestration in the  
57 ecosystem. The most widely used soil models (Century, RothC) emphasize the C flow from  
58 easily degradable to stable organic compounds using first-order kinetics to describe their decay  
59 rates (Campbell and Paustian, 2015). The relevance of chemical recalcitrance, used in those  
60 models, is accepted in the early stages of litter decomposition, but that approach has been  
61 questioned on the long term soil organic matter (SOM) stabilization (Schmidt *et al.*, 2011),  
62 highlighting the relevance of other processes in the physical protection of SOM within soil  
63 matrix (Deckmyn *et al.*, 2020). This has led to the development of models including an explicit  
64 representation of structural effects on SOM (Kuka *et al.*, 2007). Furthermore, recent studies have  
65 shown that microbial products from the transformation of plant litter are the largest contributors  
66 to stable SOM (Mambelli *et al.*, 2011; Cotrufo *et al.*, 2013).

67 The insights concerning the role of the microbial biomass in C turnover has been introduced in  
68 models such as MIneral-Microbial Carbon Stabilization (MIMICS) model (Wieder *et al.*, 2014;  
69 Wieder *et al.*, 2015) and Litter Decomposition and Leaching (LIDEL) model (Campbell *et al.*,  
70 2016). However, soil fauna and especially ecosystem engineers, i.e. organisms that create,  
71 modify or maintain habitats by changing the physical structure of the ecosystem (Jones *et al.*,  
72 1994), have also been shown to play a key role in determining C and nutrient turnover and  
73 hydrology of soils through their impact on aggregation, pore formation and bioturbation as well  
74 as their direct contribution to litter and SOM turnover (Filser *et al.*, 2016; Lavelle *et al.*, 2016).  
75 Several authors have highlighted the need to include soil fauna contributions to SOM dynamics  
76 into soil modelling (see review by Vereecken *et al.*, 2016). This information has been used in  
77 detailed and small-scale soil models (Chertov *et al.*, 2017a; Geisen *et al.*, 2019), but is not

78 incorporated into larger-scale ecosystem models. The main difficulty is the lack of data  
79 concerning the soil, either physical, chemical or biological, and the different methods used,  
80 making parameterization of any model unsure. The goal of the KEYLINK model is to consider  
81 the soil including the main mechanisms concerning the effects of soil biota on litter and SOM  
82 transformations and hydrology through structural modifications, without increasing the number  
83 of parameters beyond what is currently available on most well-measured ecosystems (Deckmyn  
84 *et al.*, 2020). We show how this model has been parameterized for a forest stand where soil fauna  
85 was never studied in detail, but many other soil and stand characteristics are well established.

86 The core model concept is the strong link between soil biota, soil structure and turnover (**Fig. 1**).  
87 The decay of fresh litter is dependent on the recalcitrance and carbon to nitrogen (N) ratio (C:N)  
88 of the litter, although different soil biota groups have specific sensibilities to recalcitrance and  
89 C:N ratio. For SOM, the turnover depends on the accessibility, linked to the pore size  
90 distribution, the aeration and H<sub>2</sub>O in the pores and the aggregation (based on the model by Kuka,  
91 Franko and Rühlmann, 2007). Both SOM and litter turnover depend on temperature and  
92 humidity. Soil fauna, specifically ecosystem engineers, directly affect pore distribution besides  
93 an important effect on bioturbation. Pore distribution affects hydrology which again affects all  
94 soil processes.

95 The scientific background for the model is fully described in Deckmyn *et al.* (2020). Here, the  
96 related processes are formulated mathematically. Finally, we show how the model can simulate  
97 several known mechanisms of soil faunal effects such as changes in litter recalcitrance affecting  
98 fungal/bacterial ratio, changes in pH affecting earthworm populations, effects of ecosystem  
99 engineers on bioturbation and hydrology, and importance of microbivores and predators in the  
100 soil fauna food web.

## 101 **Methodology**

102 The KEYLINK model has been conceptually designed integrating the structure of the soil by its  
103 porosity, the hydrology and the C cycle through the soil food web. Those key parts of the soil  
104 interact (**Fig. 1**) determining the rates of SOM stabilization and CO<sub>2</sub> emissions from soil. The  
105 functions developed to represent and simulate those processes are presented here.

106

### 107 Structural effects

108 Pore size distribution determines accessibility for trophic interactions of soil fauna and soil  
109 microorganisms (**Fig. 2**), both by size and by aeration and H<sub>2</sub>O; soil fauna changes pore size  
110 distribution and produces cracks and fissures in the soil. In the model, pore size distribution is  
111 divided into the following five categories:

- 112 • **Inaccessible pores** (< 0.1 μm in diameter): pores around inaccessible C (within the  
113 micro-aggregate, organo-clay interaction). Water is held here but is not available to plants  
114 (measured from wilting point). The volume of inaccessible pores is related to the clay  
115 content and type.
- 116 • **Bacterial pores** (0.1 – 2 μm): the pores within macro-aggregates and pores in loam,  
117 accessible only to bacteria. Engineer saprotrophs (e.g. earthworms) can also use SOM in  
118 these pores (and in the following pore categories, all except inaccessible pores) because  
119 they eat directly all soil.

- 120 • **Micropores** (2 – 30  $\mu\text{m}$ ): pores not accessible to macrofauna, mesofauna and most  
 121 predators, but accessible to microfauna bacterivores and fungivores, fungi, mycorrhiza  
 122 and bacteria. Water is held at field capacity but available to plants. In sandy soil and  
 123 within macro-aggregates ( $> 250 \mu\text{m}$ ), pores fall in this category.
- 124 • **Mesopores** (30  $\mu\text{m}$  – 1.5 mm): pores where most soil fauna can penetrate (not  
 125 macrofauna) between large macro-aggregates ( $>1 \text{ mm}$ ) or formed by fine roots.  
 126 Mesopore volume can be determined in the field from drained water capacity (but this  
 127 includes macropores). These pores are well aerated also at field capacity, but can dry out  
 128 below field capacity.
- 129 • **Macropores** ( $> 1.5 \text{ mm}$ ): cracks or biopores formed by ecosystem engineers. They are of  
 130 vital importance for soil hydrology as preferential flow through these pores has a major  
 131 impact on infiltration rate. These are the first pores to have  $\text{O}_2$  when water level is above  
 132 field capacity, but dry out quickly below field capacity.

133

134 The initial values of soil porosity in the model simulations can be calculated from measured soil  
 135 water retention curves, or even using models such as Saxton *et al.* (1986) that yield field  
 136 capacity, porosity and wilting point from the C, clay and sand contents, or using measured bulk  
 137 density ( $D_b$ ). Following Malamoud *et al.* (2009), the percentage of total porosity ( $P_{\%}$ ) can be  
 138 computed from  $D_b$  and soil particle density ( $D_s$ ) as shown in equation 2.  $D_s$  can be measured or  
 139 is calculated from  $D_m$  = soil mineral particle density ( $2.65 \text{ g cm}^{-3}$ ) and  $D_{\text{SOM}}$  = organic particle  
 140 density ( $1.35 \text{ g cm}^{-3}$ ) as:

141

$$142 \quad D_s = \frac{100}{\frac{\% \text{SOM}}{D_{\text{SOM}}} + \frac{100 - \% \text{SOM}}{D_m}} \quad (1)$$

$$143 \quad P_{\%} = \frac{D_s - D_b}{D_s} 100 \quad (2)$$

144

#### 145 Water flow

146 We advise using KEYLINK model in combination with a detailed water model including  
 147 preferential flow through macropores as well as good representation for matrix flow (s.a.  
 148 Richards' equation). However, we show in this paper how it can be used with a simpler  
 149 representation of water flow but still allowing the important dynamic interactions between pore  
 150 sizes and hydrology that are fundamental to the model. A spilling bucket approach is used at a  
 151 daily time-step, where water drains from a layer into the underlying layer when its water content  
 152 is above field capacity in the soil matrix. However, in contrast to conventional spilling bucket  
 153 models, we allow water to flow faster through macropores (before the soil matrix is saturated).  
 154 Net precipitation ( $P_{\text{net}}$ ) is calculated as:

$$155 \quad P_{\text{net}} = P - E \quad (3)$$

156 where  $P$  is precipitation ( $\text{mm day}^{-1}$ ) and  $E$  is evapotranspiration ( $\text{mm day}^{-1}$ ) from measured or  
 157 modelled data (vegetation model). Infiltration ( $I$ ) is assumed to be equal to the part of  
 158 precipitation entering the soil. Infiltration and runoff ( $P_{\text{runoff}}$ ,  $\text{mm day}^{-1}$ ) must equal  $P_{\text{net}}$ .

$$159 \quad I + P_{\text{runoff}} = P_{\text{net}} \quad (4)$$

160 Infiltration is composed of water entering the soil matrix, water filling the macropores and water  
 161 draining from macropores. Water that enters macropores remains in the macropore domain or  
 162 enters the layers below. The fraction of infiltration entering macropores depends on the surface  
 163 area of the macropores ( $SA_{\text{macro}}$ ), assumed cylindrical. Assume measured or derived maximal  
 164 infiltration rate ( $I_{\text{maxMat}}$ ,  $\text{mm day}^{-1}$ ) of the soil matrix. Maximal infiltration rate through  
 165 macropores ( $I_{\text{maxPor}}$ ,  $\text{mm day}^{-1}$ ) is calculated from the volume of the pores ( $PV_{\text{macro}}$ ), assumed not  
 166 limiting at daily scale, plus infiltration capacity of the layer (n+1) in which the macropores end.

$$167 \quad I_{\text{maxPor}} = PV_{\text{macro}} + I_{\text{maxMat}(n+1)} \quad (5)$$

168 If  $P_{\text{net}} > (I_{\text{maxPor}} + I_{\text{maxMat}})$  runoff is calculated as:

$$169 \quad P_{\text{runoff}} = P_{\text{net}} - (I_{\text{maxPor}} + I_{\text{maxMat}}) \quad (6)$$

170 after which calculations continue using  $P_{\text{net}} - P_{\text{runoff}}$  as net precipitation.

171 If  $I_{\text{maxMat}} < P_{\text{net}} < (I_{\text{maxPor}} + I_{\text{maxMat}})$  the soil matrix is filled at a rate equal to the maximum  
 172 infiltration rate, all other water is lost either through the macropores to the next layer or by filling  
 173 macropores. If  $I_{\text{maxMat}} > P_{\text{net}}$  the soil matrix is filled with water, traditional spilling bucket, but an  
 174 equivalent volume is lost through macropores to the bottom layer depending on the surface area  
 175 of the macropores. The total soil water volume of soil layer n,  $SW_n$ , is then limited by the total  
 176 pore volume of the layer and the water already filling the pores, and is calculated as:

$$177 \quad SW_n = SW_n + \min(PV_n - SW_n, I_{\text{maxmat}}(1 - SA_{\text{macro}}), P_{\text{net}}(1 - SA_{\text{macro}})) \quad (7)$$

178 For drainage (D) to the bottom layer, the spilling bucket approach is used plus a portion of water  
 179 that goes straight through the macropores, calculated from the surface area of the macropores.

$$180 \quad D_n = P_{\text{net}} SA_{\text{macro}} + P_{\text{net}} -$$

$$181 \quad \min(PV_n - SW_n, I_{\text{maxmat}}(1 - SA_{\text{macro}}), P_{\text{net}}(1 - SA_{\text{macro}})) \quad (8)$$

182 For each pore size class the fraction water filled is calculated from the water content: so always  
 183 one pore size is partially saturated and all others are either saturated or dry within one layer.

184

## 185 C flow

186 The KEYLINK model combines soil organic matter modelling with soil food web modelling.  
 187 The model conceptualized in **Figure 2** has 13 carbon pools (**Table S1.2** in **Supplemental File**  
 188 **S1**), visualised by boxes. Above and belowground litter is assumed to be provided from an  
 189 external source (*tree shoot* in **Figure 2**) not covered by this model. It could be given through  
 190 experimental data or an external model, e.g., a tree growth model that delivers the input of litter  
 191 into the litter pool. All simulations presented here were made with constant C inputs (**Table S2.6**  
 192 in **Supplemental File S2**). *Exudation* is an input of organic carbon released from roots into the  
 193 soil organic matter pool. Every live pool has a respiration rate ( $r$ ) and a turnover or death rate ( $d$ ).  
 194 On consuming a C pool, a fraction of this pool always becomes faeces and enters the SOM pool  
 195 except for the microbial pools, i.e. microbes and microbivores. SOM can be distributed in

196 different fractions, particulate organic matter (POM) and dissolved organic matter (DOM),  
 197 which can gain relevance in the addition and simulation of other nutrient cycles and processes as  
 198 leaching. However, here, as a first version of the model, we present a simplification using SOM  
 199 as a uniform pool. The growth ( $G$ ,  $\text{g C m}^{-3} \text{ day}^{-1}$ ) of a biomass pool ( $B$ ,  $\text{g C m}^{-3}$ ) is described  
 200 according to Monod kinetic,

$$201 \quad G = \sum_{n=1}^N (g_{\max} \left( \frac{S f_a}{K_s + S} \right)_n) B \quad (9)$$

202 where  $g_{\max}$  ( $\text{g C g C}^{-1} \text{ day}^{-1}$ ) is the maximal rate of growth, to which several modifiers are applied  
 203 (see descriptions below). Substrate ( $S$ ,  $\text{g C m}^{-3}$ ) is the consumable pool, litter, SOM or biomass  
 204 of soil organism ( $n$ ), that consumer pool ( $B$ ) can use but corrected by its available fraction ( $f_a$ ).  
 205 All fluxes ( $N$ ) of consumed  $C$  from each  $S$  are summed.  $K_s$  ( $\text{g C m}^{-3}$ ) is related to substrate  
 206 quality, it gives the content required to get half the maximal growth. This is not related to the  
 207 amount that will be consumed, because consumed  $C$  equals growth + faeces, but shows how  
 208 dense the material needs to be 'found' by the consumer. Available fraction of a  $S$  to a consumer  
 209 (as  $f_a$ ) is calculated using the fraction from total porosity volume that is accessible for the  
 210 consumer, by size, minus its fraction that is completely flooded or dry (see equations 14-16).  
 211 This availability introduces the concept of physical recalcitrance, highlighting the role that soil  
 212 structure plays affecting  $C$  fluxes in the soil, because SOM decomposition rates modelling use to  
 213 rely on its chemical recalcitrance, from now on referred just as 'recalcitrance'. But physical  
 214 recalcitrance has proven to be also relevant for the calculation of SOM decomposition rates (von  
 215 Lützow *et al.*, 2008), and soil matrix also affect other biotic interactions through the food web by  
 216 this availability concept.

217 Rate of increase of a population of meso- or macrofauna depends on generation time ( $r$ ,  $K$   
 218 strategies), age distribution of the population, different life stages. Models exist for only some  
 219 soil fauna species (Osler and Sommerkorn, 2007; Chertov *et al.* 2017a). To offer a solution that  
 220 can work for both the microbial biomass and the meso- and macrofauna, we use  $g_{\max}$  as equal to  
 221 the maximal rate of increase in biomass of any population,  $dB/dt = g_{\max}$  when resources are non-  
 222 limiting and assuming the population structure is stable and optimal, equal to what is often stated  
 223 as the intrinsic growth rate of a species (Birch, 1948).

224 The net rate of change of a biomass pool is the sum of growth ( $G$ ), respiration ( $R$ ) and turnover  
 225 (death,  $D_t$ ), and possibly predation ( $P_d$ ), all in  $\text{g C m}^{-3} \text{ day}^{-1}$ :

$$226 \quad \frac{dB}{dt} = G - R - D_t - P_d \quad (10)$$

227  $R$  is a function of temperature, through respiration rate ( $r$ ,  $\text{g C g C}^{-1} \text{ day}^{-1}$ ), and biomass,  
 228 assuming the same temperature sensitivity as growth; this is somewhat different to how it is seen  
 229 in many models where a food source is turned over with a specific efficiency. From a more  
 230 faunal point of view, this makes sense: a food source is 'consumed'; the consumed material is  
 231 partly excreted and partly assimilated and spent on respiration and growth (i.e. biomass  
 232 formation).

$$233 \quad R = rB \quad (11)$$

234 While the death rate  $d$  ( $\text{g C g C}^{-1} \text{ day}^{-1}$ ) is constant.

235  $D_t = dB \quad (12)$

236 Predation depends on biomass of predator or microbivore and is calculated from the growth of  
237 the predator ( $G_{\text{pred}}$ , from equation 9) plus the fraction of the prey allocated to faeces ( $f_{\text{faec}}$ ).

238  $P_{d_{\text{prey}}} = G_{\text{pred}} (1 + f_{\text{faec}}) \quad (13)$

239

#### 240 Effect of H<sub>2</sub>O

241 Drought or saturation of a pore leads to reduced availability of the C in the pore for its food web  
242 consumers. First, the overall effect of hydration is calculated as a modifier ( $m_{\text{H}_2\text{O}_{\text{tot}}}$ ) in function  
243 of volumetric soil moisture ( $V$ ) and pore volume ( $P_{\text{vol}}$ ) (after Freytag and Luttich, 1985).

244 
$$m_{\text{H}_2\text{O}_{\text{tot}}} = \begin{cases} 4 \frac{V}{P_{\text{vol}}} \left(1 - \frac{V}{P_{\text{vol}}}\right) & \text{for } \frac{V}{P_{\text{vol}}} < 0.5 \\ 1 & \text{for } \frac{V}{P_{\text{vol}}} > 0.5 \end{cases} \quad (14)$$

245 The activity is always in the pores that are not water-logged, therefore the pore size class that is  
246 partially filled with water, and the pore size above that is assumed not yet completely dry (after  
247 Kuka, Franko and Rühlmann, 2007).

248  $m_{\text{H}_2\text{O}} = \frac{P_{\text{volA}}}{P_{\text{volA}} + P_{\text{volW}}} m_{\text{H}_2\text{O}_{\text{tot}}} \quad \text{for the pores partially filled,} \quad (15)$

249  $m_{\text{H}_2\text{O}} = \frac{P_{\text{volW}}}{P_{\text{volA}} + P_{\text{volW}}} m_{\text{H}_2\text{O}_{\text{tot}}} \quad \text{for the pores one class above,} \quad (16)$

250 where  $P_{\text{volW}}$  is the water filled pore volume and  $P_{\text{volA}}$  is the aerated pore volume. The availability  
251 ( $f_a$ ) of a substrate to a consumer is defined by the inherent availability of the pore size to the  
252 consumer, multiplied with  $m_{\text{H}_2\text{O}}$ . For surface litter these calculations are not possible since the  
253 surface litter is not in the soil matrix. However, on days without precipitation, litter humidity is  
254 assumed to be related to the soil humidity below, therefore the  $m_{\text{H}_2\text{O}}$  calculated for the microbial  
255 biomass is used.

256

#### 257 Simulating the variability in $g_{\text{max}}$

258 The maximum growth of biota is influenced by different environmental factors. Each one can  
259 lead to a modifier ( $m \in [0, 1]$ ) on  $g_{\text{max}}$ . It is easy to change, add or turn off specific modifiers  
260 according to the soil studied. Here we present a modelling framework focused on abiotic controls  
261 of growth rates, but there is room for new add-ons as for example death rate modifiers as a  
262 density-dependent microbial turnover. While interaction processes affected by the demographic  
263 density of microbial communities (e.g. competition, space constraints) can play also a significant  
264 role controlling growth and decomposition rates and improve its modelling (Georgiou *et al.*,  
265 2017), our aim in this work is to link the key roles of fauna and soil structure in C cycle  
266 modelling, and together with the hydrology can simulate constraints in biotic interactions, which  
267 are also relevant controls in microbial growth and activity.

268

269 Simulating the effect of temperature (T)

270 To simulate the effect of T on growth rate through a temperature modifier ( $m_T$ ), we use a Q10-  
 271 shaped curve between maximum tolerable temperature ( $T_{max}$ ) and minimum temperature for  
 272 consumers activity ( $T_{min}$ ), set as a default at 0°C (Franko, 1989), but unlike many models, we  
 273 assume a plateau above the optimal temperature ( $T_{opt}$ ).

$$274 \quad m_T = \begin{cases} 0, & T < T_{min} \text{ or } T \geq T_{max} \\ Q^{(T - T_{opt})/10}, & T_{min} \leq T < T_{opt} \\ 1, & T_{opt} \leq T < T_{max} \end{cases} \quad (17)$$

275 However, temperature also increases respiration (R). To simulate this temperature effect, we  
 276 assume the same Q10 function but without the plateau; in this way, when T is above the  
 277 optimum, R increases while growth does not. At some point these lines will cross and cause a net  
 278 reduction in biomass.

279

280 Effect of pH on growth

281 A good example of an optional effect is the effect of pH: for a system close to a threshold,  
 282 simulating pH can be very important, assuming a good knowledge of the system. But for well-  
 283 buffered systems, it is an unnecessary increase in complexity.  $g_{max}$  decreases at low pH for  
 284 bacteria but increases for fungi (Rousk, Brookes and Bååth, 2009; Rousk et al., 2010; Rousk,  
 285 Brookes and Bååth, 2010). For this example, we put the thresholds at 8 for fungi and 3 for  
 286 bacteria, with precision of one decimal, inducing a 10 fold reduction in  $g_{max}$  for a change in pH  
 287 of 1.

$$288 \quad m_{pH} = 1 / ((pH - 8)10) \quad \text{for fungi if } pH \geq 8.1 \quad (18)$$

$$289 \quad m_{pH} = 1 / ((3 - pH)10) \quad \text{for bacteria if } pH \leq 2.9 \quad (19)$$

290 In any other case for bacteria or fungi,  $m_{pH} = 1$ , and if  $m_{pH}$  goes above 1, it is replaced by 1. For  
 291 engineer saprotrophs, their optimal  $g_{max}$  changes (becoming  $g_{maxEng}$ ) with pH (Lavelle, Chauvel  
 292 and Fragoso, 1995; Chertov *et al.*, 2017b) according to the following equation:

$$293 \quad g_{maxEng} = \begin{cases} 0, & \text{if } pH < 3 \\ \left(\frac{g_{max}}{2}\right)(pH - 3), & \text{if } 3 \leq pH < 5 \\ g_{max}, & \text{if } pH \geq 5 \end{cases} \quad (20)$$

294

295 Effect of recalcitrance and C:N on  $g_{max}$ 

296 Overall consumption of an organism that can consume different pools is computed by simply  
 297 adding them up. However, litter is not necessarily as 'palatable', depending on its C:N ratio if

298 not enough N, and on recalcitrance if low in energy, then it is needed to consume more litter,  
 299 which is calculated through modifiers  $m_{C:N}$  and  $m_{rec}$ , respectively. This is simulated by changing  
 300  $g_{max}$ . The equation for  $m_{rec}$  is not necessary and only important if enough data on litter quality is  
 301 available or the users are interested into looking into the effects of changes in litter quality. The  
 302 litter pool can be consumed by both bacteria and fungi, and of course also detritivores.  
 303 Depending on the C:N ratio, the competition between these two is different; this is simulated by  
 304 the  $g_{max}$  of the bacteria being more variable with C:N ratio. The sensitivity is described by the  
 305 parameter  $p_{mC:N}$ , between 0 and 1.

$$306 \quad \text{fungi: } m_{C:N_{fung}} = \min\left(1, \left(\frac{C:N_{fung}}{C:N_{lit}}\right)^{p_{mC:N_{fung}}}\right) \quad (21)$$

$$307 \quad \text{bacteria: } m_{C:N_{bact}} = \min\left(1, \left(\frac{C:N_{bact}}{C:N_{lit}}\right)^{p_{mC:N_{bact}}}\right) \quad (22)$$

308

309 For litter recalcitrance ( $Rec_{lit}$ ), a linear equation instead of a power is chosen so that decay of the  
 310 recalcitrant litter is 0 if  $p_{mRec} = 1$  and is unaffected if  $p_{mRec} = 0$ . The reason for choosing a  
 311 different equation than above is that constrain of labile litter decomposition by C:N ratio should  
 312 not completely stop decomposition but adjust the decomposition rate, while recalcitrant fraction  
 313 of litter could remain almost constant for long periods. The following equations determine if the  
 314 recalcitrant fraction of litter remains stable or if it is affected by decomposers partially or even  
 315 totally.

$$316 \quad \text{fungi: } m_{rec_{fung}} = \min(1, 1 - p_{mRec_{fung}} Rec_{lit}) \quad (23)$$

$$317 \quad \text{bacteria: } m_{rec_{bact}} = \min(1, 1 - p_{mRec_{bact}} Rec_{lit}) \quad (24)$$

318

319 Adding up all these modifying effects on  $g_{max}$

320 We assume a complete additivity of the effects, so the different modifiers on  $g_{max}$  are multiplied  
 321 to get the overall effect,  $m_{tot}$  in equation 25. Another optional approach could be to use only the  
 322 most limiting effect, setting  $m_{tot}$  equal to the lowest modifier and ignoring the rest.

$$323 \quad m_{tot} = m_T m_{C:N} m_{rec} m_{pH} m_{H2O} \quad (25)$$

324

325 Not assimilated C

326 The reduction in a substrate equals the growth of the consumer plus the C that goes to faeces  
 327 (excrements) and to respiration. Fraction to excrement ( $f_{faec}$ ) is a parameter of the consumer and  
 328 assumed constant. However, one consumes more and a larger fraction becomes faeces at a lower  
 329 substrate quality, for the meso- and macro fauna, because microbes do not produce excrements;  
 330 the sensitivity of  $f_{faec}$  to C:N ratio is expressed by the modifier  $m_{faec}$ . This is however only  
 331 relevant for the detritivores and engineers (equation 26) that eat SOM and litter which can  
 332 contain extremely variable amounts of nutrients; for the predators and herbivores we assume the  
 333 variability is minimal. For the microbes, it was calculated as an effect on  $g_{max}$ .

$$334 \quad f_{\text{faecEff}} = f_{\text{faec}} + m_{\text{faec}} \frac{C:N_{\text{SOM}} - C:N_{\text{eng}}}{C:N_{\text{SOM}}} f_{\text{faec}} \quad (26)$$

335

336

337 Calculations regarding engineers

338 Soil changes made by engineer species depend on their body width, but in the model this is  
 339 simplified using initial parameters for engineers' effects that must be chosen based on an average  
 340 width (see **Table S2.5** in **Supplemental File S2**); the model then simulates their daily effects  
 341 using their biomasses. Bioturbation is a function of engineer biomass ( $B_{\text{eng}}$ ,  $\text{g C m}^{-3}$ ), which  
 342 calculates organic matter moving to deeper layers: litter moving ( $\text{g C}_{\text{lit}} \text{g C}_{\text{eng}}^{-1} \text{day}^{-1}$ ) from litter  
 343 layer to end of burrow, and SOM moving by mixing of soil between layers ( $\text{g C}_{\text{SOM}} \text{g C}_{\text{eng}}^{-1} \text{day}^{-1}$ ).  
 344 In this first version of the model, with only one soil layer, bioturbation works as a C output  
 345 flow, but in future versions with more layers it could be upgraded to C flows between them.

346 Burrow volume ( $PV_{\text{B}}$ ,  $\text{l m}^{-3}$ ) is a function of engineer biomass ( $\text{g C}_{\text{eng}} \text{m}^{-3}$ ) and the ratio of pore  
 347 volume to engineer biomass ( $VE_{\text{ratio}}$ ,  $\text{l g C}_{\text{eng}}^{-1}$ ) but towards a maximum ( $PV_{\text{Bmax}}$ ,  $\text{l m}^{-3}$ ). On the  
 348 other hand, burrow turnover ( $tPV_{\text{B}}$ ) happens at a constant rate, with average burrow lifespan of  
 349 10 years; porosity decreases and burrows become mesopores.

$$350 \quad PV_{\text{B}} = \max(\min(PV_{\text{Bmax}}, VE_{\text{ratio}} B_{\text{eng}}), (PV_{\text{macro}} - PV_{\text{textmacro}})(1 - tPV_{\text{B}})) \quad (27)$$

351 where  $PV_{\text{macro}}$  is the current pore volume of the macropores and  $PV_{\text{textmacro}}$  is the textural porosity  
 352 of the macropores (see in next section). This could be improved in future versions including  
 353 perturbations as the possible effect of heavy rain.

354

355 Porosity calculations

356 The pore volume is distributed in five classes by pore size. Initial pore size distribution is given  
 357 or measured as the total pore volume ( $PV$ ,  $\text{l m}^{-3}$ ) in each class. The link between aggregation and  
 358 porosity is hard to quantify. Regelink *et al.* (2015a) showed for different soils that overall soil  
 359 porosity is the sum of the textural porosity determined by the proportion of clay, sand and silt  
 360 fractions and aggregation porosity. They conclude that micropores, which they define  $<9 \mu\text{m}$ , are  
 361 mainly situated within the aggregates, while mesopores are situated between dry-sieved  
 362 aggregates. While Regelink *et al.* (2015a) have shown that total micro and mesoporosity ( $<1000$   
 363  $\mu\text{m}$ ) increases with total aggregate content, Grosbellet *et al.* (2011) have provided evidence that  
 364 pores in the range  $30 - 300 \mu\text{m}$  decrease with aggregation. Despite of the generally lower ranges  
 365 for mesopores ( $9 - 1000 \mu\text{m}$ ) described for soil physics (Lal and Shukla, 2004; Regelink *et al.*,  
 366 2015a), here mesopores are assumed to be physically accessible to mesofauna body size (ca.  $100$   
 367  $- 2000 \mu\text{m}$ ), so we consider that mesopores ranging  $30 - 1500 \mu\text{m}$  are a reasonable compromise.  
 368 Based on that, we decided to hypothesize that aggregation increases bacterial and micro- porosity  
 369 while decreasing mesoporosity. However, we want to emphasize that further experimental  
 370 studies are needed to establish robust relationships between aggregation and pore size  
 371 distribution.

372 Aggregates are not calculated as a pool, but the effect of aggregation is included in the  
 373 calculation of porosity as described below. The following three porosities contribute to total  
 374 porosity:

- 375 • Textural porosity ( $PV_{\text{text}}$ ): measured or calculated from % clay and sand.
- 376 • Additional aggregation porosity ( $PV_{\text{Ag}}$ ): all porosity in surplus of textural, can be  
 377 estimated, for example from PTF (PedoTransfer Function) or calculated empirically from  
 378 SOM and fungal biomass, i.e. mycorrhiza and other fungi, max 2% porosity extra  
 379 (equation 29). Aggregation (Ag) is the fraction (0–1) of the SOM aggregated calculated  
 380 as (based on the data from Malamoud *et al.*, 2009):

$$381 \quad Ag = \min\left(1, \frac{c(B_{\text{fung}} + B_{\text{myc}})}{B_{\text{SOM}}}\right) \quad (28)$$

382 with an empirical parameter  $c = 10$ . The aggregation porosity is then calculated as:

$$383 \quad PV_{\text{Ag}} = k Ag B_{\text{SOM}} \quad (29)$$

384 with  $k =$  coefficient ( $2 \text{ l g C}^{-1} \text{ m}^{-3}$ ) based on empirical data (Regelink *et al.*, 2015a;  
 385 Regelink *et al.*, 2015b).

- 386 • Bioporosity ( $PV_{\text{B}}$ ): biopores created by engineers. Pore formation by engineers increases  
 387 macroporosity, increasing soil layer density, but at the same time reduces mesoporosity  
 388 as engineers push soil aside and produce casts that are denser than average soil. The  
 389 relative importance of these two effects depends on the engineers' activity patterns, and is  
 390 reflected by the parameter  $f_{\text{PV}} \in (0, 1)$ , which gives the fraction of the change in biopore  
 391 volume that increases macroporosity. Therefore, the counterpart of the biopore volume ( $1$   
 392  $- f_{\text{PV}}$ )  $PV_{\text{B}}$  is 'compensated' by a decrease in mesoporosity.

393 Conceptually, the total soil porosity is then the sum of:

$$394 \quad PV_{\text{tot}} = PV_{\text{text}} + PV_{\text{Ag}} + f_{\text{PV}}PV_{\text{B}} \quad (30)$$

395 In the model, pore volume is calculated for each pore size separately.

396 The volume of micropores ( $PV_{\text{micro}}$ ) and bacterial pores ( $PV_{\text{bact}}$ ) increases with increasing  
 397 aggregation. Apart from creating additional porosity depending on the total amount of  
 398 aggregated SOM (eq. 29), aggregation also increases the relative micro- and bacterial pore  
 399 volume at the expense of (textural) mesoporosity ( $PV_{\text{meso}}$ ), therefore not increasing total  
 400 porosity. This effect is controlled by available pore space between mineral particles (i.e. textural  
 401 mesoporosity) and we assume that half of this mesoporosity can be affected by aggregation. In  
 402 both cases, we assume that the increase in porosity due to aggregation is divided equally among  
 403 micropores and bacterial pores. The pore volume in different size classes is calculated as:

$$404 \quad PV_{\text{macro}} = PV_{\text{textmacro}} + PV_{\text{B}} \quad (31)$$

$$405 \quad PV_{\text{meso}} = PV_{\text{textmeso}} - (1 - f_{\text{PV}})PV_{\text{B}} - \frac{Ag}{2}PV_{\text{textmeso}} \quad (32)$$

$$406 \quad PV_{\text{micro}} = PV_{\text{textmicro}} + k\frac{Ag}{2}B_{\text{SOM}} + \frac{Ag}{4}PV_{\text{textmeso}} \quad (33)$$

$$407 \quad PV_{\text{bact}} = PV_{\text{textbact}} + k\frac{Ag}{2}B_{\text{SOM}} + \frac{Ag}{4}PV_{\text{textmeso}} \quad (34)$$

408 Volume of inaccessible pores is assumed to be constant and equal to  $PV_{\text{textinac}}$ .

409 These changes are calculated daily to give a dynamic feedback to the hydrology and to the  
410 distribution of each C source among pore classes, affecting its availability.

411

#### 412 Leaching

413 Water leaving one soil layer (n) is moved to the layer below (n+1). Dissolved organic and  
414 inorganic compounds are a complex matter to simulate since they are strongly dependent on the  
415 pH and the mother-material, i.e. clay and Ca rich or not. Nonetheless, in many systems  
416 simulating leaching of N and DOM is highly relevant. Unless better data are available, we  
417 suggest the following, semi-empirical method:

418 DOM can be simulated in relation to the  $\text{CO}_2$  released as total respiration ( $R_{\text{tot}}$ ,  $\text{g C m}^{-3} \text{ day}^{-1}$ )  
419 based on the consideration that high ‘activity’ in the soil is related to high  $R_{\text{tot}}$ . This is calculated  
420 as a fraction ( $f_{\text{DOM}}$ ) of  $R_{\text{tot}}$  entering the DOM pool, similar to the concepts used in the LIDEL  
421 model, in addition to the directly exuded DOM ( $C_{\text{Exud}}$ ,  $\text{g C m}^{-3} \text{ day}^{-1}$ ) which is an input (from  
422 data or a vegetation model). Assuming a short half-life of DOM and semi-empirically, because  
423 daily concentration is not ‘equal’ to daily production ( $\text{DOM}_p$ ,  $\text{g C m}^{-3} \text{ day}^{-1}$ ) but is linearly  
424 related to the daily production, we consider:

$$425 \text{DOM}_p = C_{\text{Exud}} + f_{\text{DOM}}R_{\text{tot}} \quad (35)$$

426 DOM has a short half-life but the dissolution is even faster (hours). We assume the daily  
427 concentration is in equilibrium between dissolved and adsorbed ( $\text{DOM}_{\text{ad}}$ ) depending on  
428 adsorption coefficient  $K_D$  of the soil ( $\text{m}^3 \text{ kg}^{-1} \text{ soil}$ ). Similar to the modelling in Orchidee-SOM  
429 (Cammino-Serrano *et al.*, 2018) we assume:

$$430 \text{DOM}_{\text{ad}} = K_D \text{DOM} \quad (36)$$

431 with  $K_D$  depending on the minerals and pH. More clay ( $f_{\text{Clay}}$  fraction) means less mobile DOM,  
432 and lower pH is also a cause of less mobile DOM.

$$433 K_D = a_{\text{KD}} - b_{\text{KD}}\text{pH} + c_{\text{KD}} f_{\text{Clay}} \quad (37)$$

434 with values 0.001226, 0.000212 and 0.00374 respectively for  $a_{\text{KD}}$ ,  $b_{\text{KD}}$  and  $c_{\text{KD}}$ , from Cammino-  
435 Serrano *et al.* (2018).

436 DOM leaching is calculated as the volume of water leaching to a lower layer multiplied with the  
437 concentration of dissolved DOM.

438

#### 439 Calculation order

440 The sequence of function sets used by the model to calculate all carbon fluxes and ecosystem  
441 changes is as follows:

- 442 a) Calculate the pore size fractions in 5 classes and the associated pore surface areas
- 443 b) Calculate the water volume of the relevant pore size
- 444 c) Use the precipitation leaching to calculate DOM leaching

- 445 d) Calculate for each biota group the accessibility of each of the pools it consumes
- 446 e) Calculate the  $g_{\max}$  depending on temperature,  $H_2O$ , C:N, pH and recalcitrance
- 447 f) Solve the 12 differential equations for increase/decrease of all C pools
- 448 g) Update all C pools
- 449 h) Calculate the new C:N and recalcitrance of each pool
- 450 i) Calculate engineering effect
- 451 a. Update macropores
- 452 b. Update SOM from bioturbation
- 453 j) Calculate other changes in pore size distribution from weather or management

454 The KEYLINK core model consists of steps d to i; steps a, b, c and j are add-ons that could be  
455 replaced by other models (e.g. water flow model) coupled to KEYLINK. Steps a-c are used to  
456 calculate the distribution of porosity between the pore classes, the hydrology and daily soil water  
457 content (distributed among pore classes), and then step d calculates how that is affecting the  
458 availability of each C source to its consumers. That couples soil structure and hydrology with  
459 trophic interactions, allowing the resolution of differential equations for C fluxes.

460

#### 461 Model coding and output

462 KEYLINK consists of a relatively limited, freely downloadable Python code (available at:  
463 <https://github.com/Plant-Root-Soil-Interactions-Modelling/KEYLINK>). Each of the modifiers on  
464 growth, i.e. temperature, pH,  $H_2O$ , recalcitrance and C:N, as well as the primal shape of the  
465 growth equations can be adapted towards specific questions or ecosystems. The inputs in the  
466 current version are read from data-files but are easy to link to a mechanistic model. The output of  
467 the current version consists of all daily C pools as well as the main C fluxes. KEYLINK is also  
468 available as a stand-alone executable model, allowing it to be called from models in other  
469 languages. A single run of ten years could take less than one minute (depending on computing  
470 power). In this version, the average results over one hundred runs are calculated but also all daily  
471 outputs of each run are saved.

472

#### 473 Model parameterization

474 The first version of KEYLINK model has been parameterized for a Scots pine forest stand  
475 situated in Brasschaat, in the Campine region in Belgium (51°18' N and 4°31' E) but without  
476 modelling the complete forest ecosystem (to simplify the interpretation of the results from  
477 KEYLINK). The goal of this parameterization was a model verification, not a model application  
478 for which a complete integration with an aboveground model or detailed above ground data  
479 would be necessary.

480 The soil of the Brasschaat forest is sandy but with high ground water table, so trees are generally  
481 not water-limited, but the topsoil is often dry. The soil is acidic (pH 3.5). The trees were planted  
482 around 1930 and formed a rather sparse vegetation in 1999, with leaf area index (LAI) ranging  
483 from 2.1 to 2.4.

484 For this model run, we used the following input data from the stand (**Table 1**). In this case, we  
485 did not use measured or modelled growing trees but constant input of aboveground and

486 belowground litter (measured value). The top 90 cm of soil from the Brasschaat forest was  
487 analyzed in 1999 by Janssens *et al.* Earthworm biomass, used in this case as an example of  
488 ecosystem engineers, is extremely low due to the low pH, it was not measured since 1993 by  
489 Muys, but these data are used since there is no reason to expect there was a marked change.

490 Data availability on soil pools, biology and functioning is generally low, and it is currently not  
491 possible to find a dataset describing in detail, and with small error margins, the temporal  
492 evolution of all different soil biological compartments and SOM pools. Available data are often  
493 incomplete, or based on rough estimates, e.g. from semiquantitative DNA analysis for microbial  
494 abundance in soils. To deal with this issue, a quite pragmatic approach combining different  
495 estimates from different sources is appropriate for most datasets where the soil is not the key  
496 focus, but a means to improve the simulation of an ecosystem.

497 The daily loss of water by evapotranspiration was calculated using an equation for potential  
498 evapotranspiration based on Thornthwait (1948) in this study.

#### 499 Model calibration

500 Once the model is parameterized for an ecosystem, the next step is to optimize that model,  
501 calibrating the fit of its simulations to the ecosystem data. The optimization included in the  
502 KEYLINK model follows a Bayesian procedure (Van Oijen, Rougier and Smith, 2005; Van  
503 Oijen, 2008).

504 A pragmatic assumption is that the starting values of the C pools (including the soil fauna initial  
505 biomasses) are at steady state for a given date (most often spring or summer, it would be  
506 unrealistic to keep the values constant through the year as they fluctuate with climate). The  
507 simplest calibration of any ecosystem can be done by assuming these 11 carbon pools (litter,  
508 SOM and the 9 functional groups in food web) need to be stable over the simulated years, e.g.  
509 for 9 years that gives us 99 data points by taking the same value for each C pool every year  
510 (**Table 2**). Initial litter, SOM and biomasses of bacteria, fungi and engineers were taken from the  
511 references cited in **Table 1**. For other C pools, data were estimated using measured data for  
512 previous C pools and similar proportions between C pools as in the Swedish pine forest in  
513 Persson *et al.* (1980); predator biomass was assumed to be the 20% of all biomass in their  
514 consumed C pools. Errors were assumed as a percentage of biomass, 10% for predators, 12.5%  
515 for litter and SOM, and 20% for the rest C pools.

516 It is common to apply a correction (“burn-in”) deleting part of the posterior, e.g. the first half of  
517 the runs, to avoid the effect of the starting distribution (Gelman and Shirley, 2011). For this  
518 calibration, a sample of the last one hundred accepted parameter vectors was taken from the  
519 posterior distribution, and it was used for all further model runs, so every run was performed  
520 with 100 different parameter sets.

521

#### 522 Input parameters of species

523 The KEYLINK model framework is conceptualized as an adaptable framework. Each user needs  
524 to determine for their specific site and questions the main drivers and pools required. Depending  
525 on the dataset, it is in general better to use less pools and equations if sparse data are available.  
526 Moreover, KEYLINK is not a soil fauna model and was not designed to simulate specific soil

527 fauna species in detail. The soil fauna groups used consist of a wide range of species, for which  
528 average data are used. For a description of the species categories, we refer to the review on the  
529 KEYLINK concepts (Deckmyn *et al.*, 2020).

530 Microbes and meso-macro fauna have a temperature curve using an optimum, minimum and  
531 maximum temperature. Each soil biota group also has its own maximum growth rate, C:N ratio,  
532 respiration rate and size. Death rate ( $d$ ) is the inverse of turnover, mostly given in days. In  
533 **Supplemental File S1** we briefly review main input parameters. We propose setting  $K_s$ , the  
534 concentration of the food source at which growth rate is half the maximum, equal to the existing  
535 concentrations for all meso- and macro fauna, so assuming growth could double at unlimited  
536 food source. But for microbial biomass the difference between growth of bacteria on a petri-dish  
537 unlimited in nutrients compared to field data of soil microbes clearly indicates that  $g_{max}$  in the  
538 soil is not comparable to laboratory data; if such data of  $g_{max}$  are used, the  $K_s$  should be increased  
539 considerably.

540

#### 541 Calibration for Brasschaat pine forest

542 We show here the results from a calibration towards data measured and assumed, using  
543 proportions between fauna groups in Persson *et al.* (1980), in the Brasschaat Scots pine stand in  
544 Belgium. This forest stand is relatively well described in many publications concerning the trees  
545 and the total ecosystem fluxes, but less concerning the soil and very little was measured on soil  
546 fauna. Therefore, the partially assumed data refers to a hypothetical ecosystem that does not fully  
547 fit with reality in Brasschaat forest. We use this forest as an example of how the KEYLINK  
548 model can be used to improve our understanding of the system even when detailed soil faunal  
549 data are limited.

550 The parameters  $g_{max}$ ,  $K_s$  and  $r$  are linked (increasing  $g_{max}$  has a similar effect to decreasing  $K_s$  or  
551  $r$ ). However,  $g_{max}$  or  $r$  ranges can be found in literature relatively easily. Therefore, we use fixed  
552 values for  $K_s$  (see **Supplemental File S2**) and parameterize  $g_{max}$  within the known limits. In this  
553 way, the number of parameters to be calibrated is 9, which is a reasonable number for most cases  
554 where limited data to calibrate towards are available. Of course, a user could decide to optimize  
555 more parameters if more data are available. A useful ‘rule of the thumb’ is limiting the number  
556 of parameters to the square root of the number of calibration data available (Jørgensen, 2009),  
557 which means we can get a reasonable result for nine parameters assuming 81 data points.

558 In our case, no measurements of growth rates were available and information in the literature  
559 was scant. Therefore, we deliberately defined wide ranges for the prior values of each parameter  
560 to cover all the possible values found in the literature (Chuine, 2000; Linkosalo, Lappalainen and  
561 Hari, 2008). For species for which no prior parameter information was available, we assumed  
562 parameter values equal to the mean value of the range. The initial uncertainty of each parameter  
563 is quantified in terms of a prior probability distribution with lower and upper bounds. Because of  
564 lack of detailed knowledge, we assumed the distribution as uniform and non-correlated.

565 The  $g_{max}$  values were optimized using the prior range for  $g_{max}$  (**Table 3**). The data used to  
566 calibrate against were chosen to give a ‘standard’ procedure, so limited to biomass of the  
567 different C pools. Including all available data s.a. soil respiration, soil humidity could improve  
568 the run for Brasschaat, but would not be a representative run for the model. Other parameter

569 settings, e.g. sensitivity to C:N and recalcitrance, were based on model runs of the Brasschaat  
570 site by Deckmyn *et al.* (2011).

571 We ran the model for the time period 1999-2008, because this was the period in which the forest  
572 was still clearly dominated by Scots pine; since then a transition to more deciduous trees has  
573 been taking place. We calibrated towards stable C pools over the ten years for all C pools, with  
574 an allowed error margin of 20% for all faunal pools, except 10% for predators, and 12.5% for  
575 litter and SOM. Daily climate data (temperature and precipitation) were used. The full range of  
576 input data can be found in **Supplemental File S2**, except climate data, which can be downloaded  
577 with the model. Choosing to calibrate towards one or more pools can yield different results, and  
578 it depends on the end-user's goal which calibration is preferred.

579

## 580 Model evaluation

581 Although coupling KEYLINK to real or simulated data of the aboveground ecosystem would  
582 yield more realistic results, in this exercise we used KEYLINK as a stand-alone model with quite  
583 constant input (e.g. litter, plant water uptake) to minimize the feedback effects and give a clear  
584 view on the model behaviour. This is a model evaluation, not a full model validation.

585 After calibration to the Brasschaat dataset, a set of scenarios was performed to evaluate the  
586 model: I. Basic results; II. Sensitivity to initial soil structure; III. Changing initial litter C:N ratio;  
587 IV. Changing initial litter recalcitrance; V. Changing soil pH; VI. Excluding predators.

588 Scenario I was done with the reference input parameters (**Supplemental File S2**), and used as a  
589 basal one to be compared with the other five alternative scenarios: scenario II with higher clay  
590 content in the soil (clay 15%); scenario III with lower litter C:N ratio (40); scenario IV with  
591 lower litter recalcitrance (20%); scenario V with higher pH (5.9); and scenario VI without  
592 predators by setting its initial biomass to 0 ( $B_{pred} = 0$ ).

593 In each one of the five alternative scenarios, input parameters were the same than in the basal  
594 scenario, except for the parameter changed to generate the new scenario (see **Supplemental File**  
595 **S2**). All the six scenarios were run 100 times using a sample of 100 parameter vectors from the  
596 posterior distribution of the calibration, consisting each run in a simulation of 10 years at a daily  
597 time-step (3653 days). Then, averages of biomasses were calculated for each C pool among the  
598 100 simulations of 10 years, for each scenario, comparing the effects of disturbances on average  
599 values.

600

## 601 **Results**

### 602 Calibration

603 The model was run ca. 100000 times with different parameter settings sampled from the prior  
604 parameter distribution. A sample of the posterior distribution was taken with the last 100  
605 accepted parameter vectors for  $g_{max}$  (**Table 4**).

606 The optimization showed the link between the different groups of soil biota, e.g. a high  $g_{max}$  for  
607 bacteria was coupled to a high  $g_{max}$  for bacterivores. The alternative five scenarios compared to

608 the basal one can show very different results concerning specific C pools (**Table 5**). Running the  
609 model 100 times using the sample of the  $g_{\max}$  values resulted in predictions with a quite wide  
610 range (**Table 6**).

#### 611 Basic results

612 Mycorrhiza, herbivores and detritivores are relatively uncoupled, though influenced by  
613 predators, and follow the yearly climate curves. The bacterial and fungal biomasses are very  
614 strongly linked. The high  $g_{\max}$  of bacteria allows steep peaks, which are generally followed by  
615 peaks in bacterivore biomass. As we used constant litter input into the soil and used a calculated  
616 constant fraction of potential evapotranspiration as water uptake from the soil, it cannot be  
617 expected that these results follow the normal annual trends in fluctuations of those fluxes. This  
618 can, at least partially, explain the relatively low bacterial biomass found in our results, since the  
619 bacteria would profit most from a rapidly changing environment, but under some unrealistic  
620 simulated conditions fungi could be displacing bacteria by competitive exclusion. For more  
621 realistic simulations the model can be coupled with other models that give that information as  
622 outputs, or with measured datasets.

623 All C pools tend to reach some stability after the first years, suggesting the model is well-  
624 balanced; however, stability values seem to be more sensitive to changes in  $g_{\max}$  parameters for  
625 some pools (e.g. SOM). The set-up of the model, where we only calibrate the faunal  $g_{\max}$ , does  
626 not allow calibration towards different ratio of litter and SOM decay. This depends on the  
627 uncalibrated parameter fragmentation, the sensitivity to recalcitrance, but also the temperature  
628 used for the litter and SOM. Here we used the same temperature, while in reality it would be  
629 expected that there would be certain differences in mean temperatures or their variability at  
630 different depths.

631 There was a high variability within the 100 simulations of each scenario, e.g. basal scenario (**Fig.**  
632 **3**), calling into question the reliability of predictions. We suggest here some theoretical  
633 predictions based on this example, but it is clear that for a realistic application it will be  
634 necessary to improve the calibration, by using more detailed data or by linking the model to a  
635 vegetation model. This highlights the relevance of developing databases including enough details  
636 for the key parameters of the different parts of the soil system (i.e. soil structure, hydrology, food  
637 webs).

638 An overview of all C pools under the different simulation scenarios (**Fig. 4**) shows how changing  
639 one input parameter at a time influences the results. It must be taken into account that KEYLINK  
640 was run as a stand-alone model, which can explain why some of the resulting outputs seem not  
641 very realistic; linking it to a model or more detailed data of the aboveground ecosystem would  
642 greatly influence the results, but would not allow clear interpretation of the model functioning  
643 due to feedbacks. Since our goal here was to introduce the belowground model itself rather than  
644 a realistic application to a particular case, we chose to avoid those feedbacks with other parts of  
645 the ecosystem that are required for more realistic simulations. To further elucidate these effects  
646 and to show some of the potential outputs the model can give, we show a few of the most  
647 interesting fluxes (**Table 7**).

648 The simulated scenarios showed that increasing clay content (i.e. changing initial soil structure)  
649 resulted in an increase in water content (**Fig. 5**) and a decrease in litter and SOM decay while  
650 fungal/bacterial ratio decreased. In fact, this scenario caused the largest change in soil water

651 content, showing the sensitivity of the system to initial soil structure and its crucial role for soil  
652 hydrology. On the other hand, lowering litter recalcitrance or C:N ratio resulted in an increase in  
653 microbial biomass, mainly fungi, which caused an increase in litter decay, while SOM decay did  
654 not show a clear change. The scenario with higher pH allowed engineer species (and predators  
655 with them) to increase in biomass, altering the soil structure with an increase in macroporosity,  
656 which caused a clear decrease in SOM stabilization. Finally, the exclusion of predators totally  
657 changed the soil porosity and the trophic interactions along the food web, causing the largest  
658 increase in the decay of SOM and litter, which highlights the crucial role of predators in the  
659 regulation of the soil C cycle.

660

661

## 662 **Discussion**

663 The Brasschaat forest is sandy, with low pH and recalcitrant litter; as expected, this is an  
664 environment not suited to earthworms. The model correctly simulated extremely low values of  
665 engineer biomass. Increasing the pH increased the engineers pool, e.g. earthworms population,  
666 but this remained too low to have a significant impact on the system. This is quite realistic as  
667 neither litter quality nor soil quality are ideal for earthworms. Obviously, to calibrate the specific  
668 parameters concerning earthworms the Brasschaat forest is not an ideal site.

669 The high variability observed in some populations could make them appear more unstable than  
670 what can be expected in reality, and it is indeed expectable that a more realistic application of the  
671 model will yield different results. However, there are also empirical evidences that some  
672 populations, e.g. microbial biomasses, can be very unstable depending on hydrology (Blackwell  
673 *et al.*, 2010; Zhao *et al.*, 2010), showing short-term spikes in biomass as those observed in the  
674 presented simulations, in response to predicted changes in water availability.

675 Changes in litter quality (i.e. in C:N ratio and recalcitrance) caused small differences between  
676 scenarios, being the simulations from those two alternative scenarios quite similar to the basal  
677 scenario. Despite the apparent increase in litter decay for lower litter recalcitrance and for lower  
678 C:N ratio, as mentioned before, the high variability among simulations (**Fig. 3**) suggests that  
679 differences between scenarios caused by changes in litter quality are negligible. It is well known  
680 that litter quality is one of the main factors controlling litter decomposition rates (Zhang *et al.*,  
681 2008; García-Palacios *et al.*, 2013), and the observed trend fits with experimental evidence, but  
682 clearer effects of changes in litter quality are expected. Therefore, these simulations should be  
683 tested again, particularly with the model linked to a vegetation model, and, if necessary,  
684 improvements should be added.

685 Changes in textural porosity, on the other hand, showed clearer effects on soil processes. The  
686 scenario changing clay content to increase textural porosity caused the highest impact on  
687 hydrology, increasing soil water content (E in **Figure 5**), which led to a decrease in SOM  
688 availability, decreasing microbial community biomasses and, therefore, decreasing the  
689 decomposition of SOM and litter. However, changes in C pools were not as clear as in  
690 hydrology, mainly due to the high uncertainty in calibration results.

691 The scenario without predators showed the most interesting results because the interactions  
692 between the different food web parts are apparent, and it showed a high contrast with the basal

693 scenario. Exclusion of predators, setting the starting biomass of that pool at 0, showed how the  
694 model tracks its crucial role in the ecosystem (**Fig. 4**). Predators produce a top-down trophic  
695 cascade on the food web, e.g. on herbivores and roots. Microbial decay is reduced as fungi and  
696 bacteria are consumed by the increased populations of bacterivores and fungivores. Despite of  
697 the decrease in bacteria and fungi, SOM and litter were also lower without predators. This could  
698 be explained by an increase in engineer populations with implications also on the soil matrix.  
699 Overall the model successfully tracked soil food web dynamics and also their interactions with  
700 soil porosity. The effect of larger soil predators (e.g. Araneae, Carabidae, Formicidae) slowing  
701 down SOM decomposition and enhancing its stabilization has been previously found in  
702 experiments (Kajak, 1995), as well as mycorrhiza effect on porosity by making aggregates  
703 (Siddiky *et al.*, 2012). Those trophic cascade effects over SOM stabilization depends on  
704 environmental conditions such as rainfall, with predation on microbivores reducing litter  
705 decomposition rates in more humid sites, while reductions in rainfall could lead to a shift in that  
706 trend with predation on microbivores indirectly increasing litter decomposition rates (Lensing  
707 and Wise, 2006). The predicted effects of predator exclusion increasing SOM and litter decay  
708 have been found in different ecosystems, e.g. grasslands (Kajak, 1997) and forests (Lawrence  
709 and Wise, 2000), but contrasting results (e.g. Kajak, 1995; Lawrence and Wise, 2004) suggest  
710 that it is not a general pattern. Considering the high rainfall conditions at the modelled Belgian  
711 forest, and according to the suggested trends based on experimental research, soil predators  
712 feeding on microbivores at Brasschaat forest could promote SOM stabilization, which would fit  
713 with the simulated scenarios. Therefore, KEYLINK model seems to fit with the expected food  
714 web and C dynamics, and could serve to improve the biogeochemical cycles modelling, as is  
715 needed for larger scale predictions (Grandy *et al.*, 2016), by coupling it with other ecosystem  
716 models.

717 Hydrology is influenced by aggregation and by macropore formation by ecosystem engineers.  
718 The increased macroporosity increases infiltration rate with reduced water-logging and runoff.  
719 Predators have a clear indirect effect on soil porosity by consuming engineer species, and also  
720 microbivore species, which leads to changes in soil hydrology (**Fig. 5**). Variations in bacterial  
721 pore and micropore volume are positively correlated, while mesopore variations are negatively  
722 correlated with both; the higher volume in mesopores, the lower in the two other classes, and the  
723 faster the water drains from the soil layer. That is what we can expect to happen in real soils, so  
724 the model seems to simulate appropriately those dynamics. The increase in macro and  
725 mesoporosity volumes without predators, so with higher engineers, resulted in a decrease of soil  
726 water content of 9.26 % (increasing the pore aeration), and under those conditions the  
727 availability of SOM and litter for bacteria and fungi could be increased, explaining why SOM  
728 and litter are lower even with lower bacteria and fungi. This highlights the role of hydrology on  
729 trophic cascade processes, which can be enhanced or reduced by water distribution through the  
730 soil matrix (Erktan, Or and Scheu, 2020), and also the relevance of considering how climate  
731 change effects on soil structure, hydrology and food web interactions (particularly trophic  
732 cascades) can affect microbial communities (Thakur and Geisen, 2019) and, therefore, litter and  
733 SOM decomposition.

734 The aim of this study was to present a first version of a new concept model that hopefully will  
735 serve to challenge current state-of-the-art soil modelling. But we are aware that to do that we will  
736 need to improve the calibration of the model in the future, using more complete databases that  
737 take into account all the elements needed to calibrate KEYLINK, which, on the other hand, are

738 currently extremely scarce. By presenting this concept model that challenges the current way of  
739 simulating soil biochemical cycling, we hope to stimulate that future studies will also be  
740 designed to take into account the pools and functional groups needed to calibrate KEYLINK.

741

## 742 **Conclusions**

743 KEYLINK is a relatively simple, fast and easy to modify soil model that can be used as a stand-  
744 alone model to understand soil systems, or linked to detailed aboveground data/models to predict  
745 SOM turnover. Model evaluation showed that KEYLINK is capable of simulating properly not  
746 only the soil food web and C pools dynamics, but also how they interact with soil porosity and  
747 hydrology, which is one of the main goals of this new model. The results from the evaluation  
748 scenarios showed that SOM turnover is driven not only by microbial biomass, but also by soil  
749 structure and hydrology. Moreover, microbial biomass is strongly regulated by the  
750 presence/absence of the other soil fauna. Especially the effects of the predators and the  
751 ecosystem engineers are extremely significant for our understanding of soil functioning.  
752 Furthermore, since management can differentially affect the larger soil fauna, KEYLINK can be  
753 of great use to investigate potential effects of management changes on soil SOM, nutrient  
754 turnover and hydrology.

755 This model shows degradability of SOM can be adequately simulated from accessibility in  
756 relation to pore space instead of the existing concepts of slow and fast pools. This allows a closer  
757 link to the soil structure and soil fauna which we consider closer to the actual, and follows the  
758 concepts as first described by Kuka, Franko and Rühlmann (2007), but applied here in a wider  
759 framework and including the hydrology.

760 For a full validation or better calibration of the model, datasets are required including basic data  
761 on the aboveground, e.g. litter input, water uptake, root growth and turnover, in combination  
762 with relatively detailed data on soil structure, i.e. pore size distribution, and hydrology and soil  
763 biota, e.g. biomass of bacteria, fungi, mycorrhizal fungi and main meso- and macrofauna. All  
764 these data are available, but very seldom at one site as most studies are focused on one or other  
765 aspect of soil science.

766 In conclusion, KEYLINK is a step towards a new generation of ecosystems models that include  
767 functional diversity, trophic structures and ecological processes as important factors shaping  
768 soil/ecosystem carbon and water cycling. Future versions, fed by more detailed data, will need to  
769 be developed in order to improve our current predictive capacity.

770

## 771 **Acknowledgements**

772 The authors express their gratitude to all the people who have contributed to the BioLink and  
773 KEYSOM COST Actions, whose work contributed also to the development of the KEYLINK  
774 model.

775

## 776 **References**

- 777 Birch, L. (1948). The intrinsic rate of natural increase of an insect population. *The Journal of*  
778 *Animal Ecology*, 17(1), 15-26.
- 779 Blackwell, M. S. A., Brookes, P. C., de La Fuente-Martinez, N., Gordon, H., Murray, P. J.,  
780 Snars, K. E., Williams, J. K., Bol, R., and Haygarth, P. M. (2010). Phosphorus  
781 solubilization and potential transfer to surface waters from the soil microbial biomass  
782 following drying–rewetting and freezing–thawing. In *Advances in agronomy* (Vol. 106,  
783 pp. 1-35). Academic Press.
- 784 Camino-Serrano, M., Guenet, B., Luysaert, S., Ciais, P., Bastrikov, B., De Vos, B., Gielen, B.,  
785 Gleixner, G., Jornet-Puig, A., Kaiser, K., Kothawala, D., Lauerwald, R., Peñuelas, J.,  
786 Schrumpf, M., Vicca, S., Vuichard, N., Walmsley, D., and Janssens, I. A. (2018).  
787 ORCHIDEE-SOM: modeling soil organic carbon (SOC) and dissolved organic carbon  
788 (DOC) dynamics along vertical soil profiles in Europe. *Geoscientific Model*  
789 *Development*, 11(3), 937-957.
- 790 Campbell, E. E., Parton, W. J., Soong, J. L., Paustian, K., Hobb, N. T., and Cotrufo, M. F.  
791 (2016). Using litter chemistry controls on microbial processes to partition litter carbon  
792 fluxes with the Litter Decomposition and Leaching (LIDEL) model. *Soil Biology and*  
793 *Biochemistry*, 100, 160-174.
- 794 Campbell, E. E., and Paustian, K. (2015). Current developments in soil organic matter modeling  
795 and the expansion of model applications: a review. *Environmental Research Letters*,  
796 10(12), 123004.
- 797 Chertov, O., Komarov, A., Shaw, C., Bykhovets, S., Frolov, P., Shanin, V., Grabarnik, P.,  
798 Pripitina, I., Zubkova, E., and Shashkov, M. (2017a). Romul\_Hum - A model of soil  
799 organic matter formation coupling with soil biota activity. II. Parameterisation of the soil  
800 food web biota activity. *Ecological Modelling*, 345, 140-149.
- 801 Chertov, O., Shaw, C., Shashkov, M., Komarov, A., Bykhovets, S., Shanin, V., Grabarnik, P.,  
802 Frolov, P., Kalinina, O., Pripitina, I., and Zubkova, E. (2017b). Romul\_Hum model of  
803 soil organic matter formation coupled with soil biota activity. III. Parameterisation of  
804 earthworm activity. *Ecological Modelling*, 345, 140-149.
- 805 Christian, P. R., and Casella, G. (1999). Monte Carlo statistical methods. Springer. New York.
- 806 Chuine, I. (2000). A unified model for budburst of trees. *Journal of Theoretical Biology*, 207(3),  
807 337-347.
- 808 Cotrufo, M. F., Wallenstein, M. D., Boot, C. M., Deneff, K., and Paul, E. (2013). The Microbial  
809 Efficiency-Matrix Stabilization (MEMS) framework integrates plant litter decomposition  
810 with soil organic matter stabilization: do labile plant inputs form stable soil organic  
811 matter? *Global Change Biology*, 19, 988-995.
- 812 Deckmyn, G., Campioli, M., Muys, B., and Kraigher, H. (2011). Simulating C cycles in forest  
813 soils: Including the active role of micro-organisms in the ANAFORE forest  
814 model. *Ecological Modelling*, 222, 1972-1985.

- 815 Deckmyn, G., Meyer, A., Smits, M. M., Ekblad, A., Grebenc, T., Komarov, A., and Kraigher,  
816 H., (2014). Simulating ectomycorrhizal fungi and their role in carbon and nitrogen  
817 cycling in forest ecosystems. *Canadian Journal of Forest Research*, 44(6), 535-553.
- 818 Erktan, A., Or, D., and Scheu, S. (2020). The physical structure of soil: Determinant and  
819 consequence of trophic interactions. *Soil Biology and Biochemistry*, 107876.
- 820 Filser, J., Faber, J. H., Tiunov, A. V., Brussaard, L., Frouz, J., De Deyn, G., Uvarov, A.  
821 V., Berg, M. P., Lavelle, P., Loreau, M., Wall, D. H., Querner, P., Eijsackers,  
822 H., and Jiménez, J. J. (2016). Soil fauna: key to new carbon models. *Communications in  
823 Soil Science and Plant Analysis*, 2, 565-582.
- 824 Franko, U. (1989). C-und N-Dynamik beim Umsatz organischer Substanzen im Boen. Diss.,  
825 Berlin, Akad. Landwirtsch.
- 826 Freytag, H. E., and Luttich, M. (1985). Zum Einfluß der Bodenfeuchte auf die Bodenatmung  
827 unter Einbeziehung der Trockenraumdichte. *Archiv für Acker-und Pflanzenbau und  
828 Bodenkunde*, 29(8), 485-492.
- 829 García-Palacios, P., Maestre, F. T., Kattge, J., and Wall, D. H. (2013). Climate and litter quality  
830 differently modulate the effects of soil fauna on litter decomposition across  
831 biomes. *Ecology letters*, 16(8), 1045-1053.
- 832 Gaublonne, E., De Vos, B., and Cools, N. (2006). An indicator for microbial biodiversity in  
833 forest soils. *Brussels (BE): Instituut voor Natuur-en Bosonderzoek (INBO)*. R.
- 834 Geisen, S., Briones, M. J., Gan, H., Behan-Pelletier, V. M., Friman, V.P., de Groot, G. A.,  
835 Hannula, S. E., Lindo, Z., Philippot, L., Tiunov, A. V., and Wall, D. H. (2019). A  
836 methodological framework to embrace soil biodiversity. *Soil Biology and Biochemistry*,  
837 136, 107536.
- 838 Gelman, A., and Shirley, K. (2011). Inference from simulations and monitoring convergence. In:  
839 Brooks, S., Gelman, A., Jones, G., and Meng, X. L. (eds.), *Handbook of Markov Chain  
840 Monte Carlo*, 6, 163-174. CRC press, USA.
- 841 Georgiou, K., Abramoff, R. Z., Harte, J., Riley, W. J., and Torn, M. S. (2017). Microbial  
842 community-level regulation explains soil carbon responses to long-term litter  
843 manipulations. *Nature Communications*, 8(1), 1-10.
- 844 Grandy, A. S., Wieder, W. R., Wickings, K., and Kyker-Snowman, E. (2016). Beyond microbes:  
845 Are fauna the next frontier in soil biogeochemical models? *Soil Biology and  
846 Biochemistry*, 102, 40-44.
- 847 Grosbellet, C., Vidal-Beaudet, L., Caubel, V., and Charpentier, S. (2011). Improvement of soil  
848 structure formation by degradation of coarse organic matter. *Geoderma*, 162(1-2), 27-38.
- 849 Horemans, J., Roland, M., Janssens, I., and Ceulemans, R. (2017). Explaining the inter-annual  
850 variability in the ecosystem fluxes of the Brasschaat Scots pine forest: 20 years of eddy  
851 flux and pollution monitoring. In: *EGU General Assembly Conference Abstracts*, 19,  
852 10402.

- 853 Janssens, I. A., Sampson, D. A., Cermak, J., Meiresonne, L., Riguzzi, F., Overloop, S., and  
854 Ceulemans, R. (1999). Above- and belowground phytomass and carbon storage in a  
855 Belgian Scots pine stand. *Annals of Forest Science* 56, 81-90.
- 856 Janssens, I. A., Sampson, D. A., Curriel Yuste, J., Carrara, A., and Ceulemans, R. (2002). The  
857 carbon cost of fine root turnover in a Scots pine forest. *Forest Ecology and Management*,  
858 168(1-3), 231-240.
- 859 Jones, C. G., Lawton, J. H., and Shachack, M. (1994). Organisms as ecosystem engineers. *Oikos*  
860 69, 373-386.
- 861 Jørgensen, S. E. (2009). *Ecological modelling: an introduction*. WIT press. ISBN 978-1-84564-  
862 408-6
- 863 Kajak, A. (1995). The role of soil predators in decomposition processes. *European Journal of*  
864 *Entomology*, 92(3), 573-580.
- 865 Kajak, A. (1997). Effects of epigeic macroarthropods on grass litter decomposition in mown  
866 meadow. *Agriculture, ecosystems & environment*, 64(1), 53-63.
- 867 Kuka, K., Franko, U., and Rühlmann, J. (2007). Modelling the impact of pore space distribution  
868 on carbon turnover. *Ecological Modelling*, 208(2-4), 205-306.
- 869 Lal, R., and Shukla, M. K. (2004). *Principles of soil physics*. CRC Press.
- 870 Lavelle, P., Chauvel, A., and Fragoso, C. (1995). Faunal activity in acid soils. In *Plant-Soil*  
871 *Interactions at Low pH: Principles and Management* (pp. 201-211). Springer, Dordrecht.
- 872 Lavelle, P., Spain, A., Blouin, M., Brown, G., Decaëns, T., Grimaldi, M., Jiménez, J. J., McKey,  
873 D., Mathieu, J., Velasquez, E., and Zangerlé, A. (2016). Ecosystem engineers in a self-  
874 organized soil: a review of concepts and future research questions. *Soil Science*, 181(3/4),  
875 91-109.
- 876 Lawrence, K. L., and Wise, D. H. (2000). Spider predation on forest-floor Collembola and  
877 evidence for indirect effects on decomposition. *Pedobiologia*, 44(1), 33-39.
- 878 Lawrence, K. L., and Wise, D. H. (2004). Unexpected indirect effect of spiders on the rate of  
879 litter disappearance in a deciduous forest. *Pedobiologia*, 48(2), 149-157.
- 880 Lensing, J. R., and Wise, D. H. (2006). Predicted climate change alters the indirect effect of  
881 predators on an ecosystem process. *Proceedings of the National Academy of*  
882 *Sciences*, 103(42), 15502-15505.
- 883 Linkosalo, T., Lappalainen, H., and Hari, P. (2008). A comparison of phenological models of  
884 leaf bud burst and flowering of boreal trees using independent observations. *Tree*  
885 *Physiology*, 28(12), 1873-1882.
- 886 Malamoud, K., McBratney, A. B., Minasny, B., and Field, D. J. (2009). Modelling how carbon  
887 affects soil structure. *Geoderma*, 149, 19-26.
- 888 Mambelli, S., Bird, J. A., Gleixner, G., Dawson, T. E., and Torn, M. S. (2011). Relative  
889 contribution of foliar and fine root pine litter to the molecular composition of soil organic  
890 matter after in situ degradation. *Organic Geochemistry*, 42, 1099-1108.

- 891 Muys, B. (1993). A synecological evaluation of the earthworm activity and litter decomposition  
892 in Flemish forests in the context of sustainable forest management. D. Phil. Thesis,  
893 University of Ghent.
- 894 Osler, G. H., and Sommerkorn, M. (2007). Toward a complete soil C and N cycle: incorporating  
895 the soil fauna. *Ecology*, 88(7), 1611-1621.
- 896 Persson, T., Bååth, E., Clarholm, M., Lundkvist, H., Soderstroem, B. E., and Sohlenius, B.  
897 (1980). Trophic structure, biomass dynamics and carbon metabolism of soil organisms in  
898 a Scots pine forest. *Ecological Bulletins*, 32, 419-459.
- 899 Regelink, I. C., Stoof, C. R., Rouseva, S., Weng, L., Lair, G. J., Kram, P., Nikolaidis, N. P.,  
900 Kercheva, M., Banwart, S., and Comans, R. N. J. (2015a). Linkages between aggregate  
901 formation, porosity and soil chemical properties. *Geoderma* 247, 24-37.
- 902 Regelink, I. C., Weng, L., Lair, G. J., and Comans, R. N. J. (2015b). Adsorption of phosphate  
903 and organic matter on metal (hydr)oxides in arable and forest soil: a mechanistic  
904 modelling study. *European Journal of Soil Science*, 66(5), 867-875.
- 905 Rousk, J., Bååth, E., Brookes, P. C., Lauber, C. L., Lozupone, C., Caporaso, J. G., Knight, R.,  
906 and Fierer, N. (2010). Soil bacterial and fungal communities across a pH gradient in an  
907 arable soil. *The ISME journal*, 4(10), 1340-1351.
- 908 Rousk, J., Brookes, P. C., and Bååth, E. (2009). Contrasting soil pH effects on fungal and  
909 bacterial growth suggest functional redundancy in carbon mineralization. *Applied and  
910 Environmental Microbiology*, 75(6), 1589-1596.
- 911 Rousk, J., Brookes, P. C., and Bååth, E. (2010). Investigating the mechanisms for the opposing  
912 pH relationships of fungal and bacterial growth in soil. *Soil Biology and  
913 Biochemistry*, 42(6), 926-934.
- 914 Saxton, K. E., Rawls, W., Romberger, J. S., and Papendick, R. I. (1986). Estimating generalized  
915 soil-water characteristics from texture 1. *Soil Science Society of America Journal*, 50(4),  
916 1031-1036.
- 917 Schmidt, M. W. I., Torn, M. S., Abiven, S., Dittmar, T., Guggenberger, G., Janssens, I. A.,  
918 Kleber, M., Kögel-Knabner, I., Lehmann, J., Manning, D. A. C., Nannipieri, P., Rasse, D.  
919 P., Weiner, S., and Trumbore, S. E. (2011). Persistence of soil organic matter as an  
920 ecosystem property. *Nature*, 478, 49-56.
- 921 Siddiky, R. K., Kohler, J., Cosme, M., and Rillig, M. C. (2012). Soil biota effects on soil  
922 structure: interactions between arbuscular mycorrhizal fungal mycelium and collembola.  
923 *Soil Biology and Biochemistry*, 50, 33-39.
- 924 Thakur, M. P., and Geisen, S. (2019). Trophic regulations of the soil microbiome. *Trends in  
925 microbiology*, 27(9), 771-780.
- 926 Thornthwait, C. W. (1948). An approach toward a rational classification of climate.  
927 *Geographical Review*, 38(1), 55-94.
- 928 Van Oijen, M. (2008). Bayesian Calibration (BC) and Bayesian Model Comparison (BMC) of  
929 process-based models: Theory, implementation and guidelines.

- 930 Van Oijen, M., Rougier, J., and Smith, R. (2005). Bayesian calibration of process-based forest  
931 models: bridging the gap between models and data. *Tree Physiology*, 25(7), 915-927.
- 932 Vereecken, H., Schnepf, A., Hopmans, J. W., Javaux, M., Or, D., Roose, T., Vanderborght, J.,  
933 Young, M. H., Amelung, W., Aitkenhead, M., Allison, S. D., Assouline, S., Baveye, P.,  
934 Berli, M., Brüggemann, N., Finke, P., Flury, M., Gaiser, T., Govers, G., Ghezzehei, T.,  
935 Hallett, P., Hendricks Franssen, H. J., Heppell, J., Horn, R., Huisman, J. A., Jacques, D.,  
936 Jonard, F., Kollet, S., Lafolie, F., Lamorski, K., Leitner, D., McBratney, A., Minasny, B.,  
937 Montzka, C., Nowak, W., Pachepsky, Y., Padarian, J., Romano, N., Roth, K., Rothfuss,  
938 Y., Rowe, E. C., Schwen, A., Šimůnek, J., Tiktak, A., Van Dam, J., van der Zee, S. E. A.  
939 T. M., Vogel, H. J., Vrugt, J. A., Wöhling, T., and Young, I. M. (2016). Modeling soil  
940 processes: Review, key challenges, and new perspectives. *Vadose Zone Journal*, 15(5).
- 941 von Lützow, M., Kögel-Knabner, I., Ludwig, B., Matzner, E., Flessa, H., Ekschmitt, K.,  
942 Guggenberger, G., Marschner, B., and Kalbitz, K. (2008). Review Article Stabilization  
943 mechanisms of organic matter in four temperate soils: Development and application of a  
944 conceptual model. *Journal of Plant Nutrition and Soil Science*, 171(1), 111-124.
- 945 Wieder, W. R., Grandy, A. S., Kallenbach, C. M., and Bonan, G. B. (2014). Integrating  
946 microbial physiology and physio-chemical principles in soils with the MIMICs-MINeral  
947 Carbon Stabilization (MIMICS) model. *Biogeosciences*, 11, 3899-3917.
- 948 Wieder, W. R., Grandy, A. S., Kallenbach, C. M., Taylor, P. G., and Bonan, G. B. (2015).  
949 Representing life in the Earth system with soil microbial functional traits in the MIMICS  
950 model. *Geoscientific Model Development Discussions*, 8(2), 1789-1808.
- 951 Zhang, D., Hui, D., Luo, Y., and Zhou, G. (2008). Rates of litter decomposition in terrestrial  
952 ecosystems: global patterns and controlling factors. *Journal of Plant Ecology*, 1(2), 85-  
953 93.
- 954 Zhao, B., Chen, J., Zhang, J., and Qin, S. (2010). Soil microbial biomass and activity response to  
955 repeated drying–rewetting cycles along a soil fertility gradient modified by long-term  
956 fertilization management practices. *Geoderma*, 160(2), 218-224.

**Table 1** (on next page)

Initial input data.

Data from Brasschaat Scots pine forest (Belgium). Microbial C pool was estimated as hot water extractable C (HWC).

| Variable              | Unit                                   | Value   | Reference                                     |
|-----------------------|--|---------|---|
| Earthworm biomass     | g C m <sup>-3</sup>                    | 200     | Muys (1993)                                   |
| pH                    |  | 3.5     | Janssens <i>et al.</i> (1999)                 |
| Sand                  | %                                      | 93      | Janssens <i>et al.</i> (1999)                 |
| Initial SOM           | g C m <sup>-3</sup>                    | 11470   | Janssens <i>et al.</i> (1999)                 |
| Initial litter        | g C m <sup>-3</sup>                    | 2680    | Janssens <i>et al.</i> (1999)                 |
| Fine root biomass     | g C m <sup>-3</sup>                    | 400     | Janssens <i>et al.</i> (2002)                 |
| Fine root litter      | g C m <sup>-3</sup>                    | 300     | Janssens <i>et al.</i> (1999)                 |
| Fine root growth rate | g C m <sup>-3</sup> year <sup>-1</sup> | 210     | Janssens <i>et al.</i> (2002)                 |
| Annual litter fall    | g C m <sup>-3</sup> year <sup>-1</sup> | 400     | Horemans <i>et al.</i> (2017)                 |
| Fine root turnover    | g C m <sup>-3</sup> year <sup>-1</sup> | 740     | Based on Janssens <i>et al.</i> (2002)        |
| C input to mycorrhiza | g C m <sup>-3</sup> year <sup>-1</sup> | 197     | Assumed based on Deckmyn <i>et al.</i> (2014) |
| Microbial C as HWC    | g m <sup>-3</sup>                      | 1338.21 | Gaublomme <i>et al.</i> (2006)                |

1

**Table 2** (on next page)

Calibration data.

Data of C pools used for the model calibration. Biomasses of the nine food web functional groups: bacteria ( $B_b$ ), fungi ( $B_f$ ), mycorrhiza ( $B_{myc}$ ), bacterivores ( $B_{bvores}$ ), fungivores ( $B_{fvores}$ ), detritivores ( $B_{det}$ ), engineers ( $B_{eng}$ ), herbivores ( $B_{hvores}$ ) and predators ( $B_{pred}$ ); and the other two C pools: litter and soil organic matter (SOM). Values were used once per year during calibration at days 180, 545, 910, 1275, 1640, 2005, 2370, 2735 and 3100.

| <b>C pool</b>             | <b>Value (g C m<sup>-3</sup>)</b> | <b>Error (g C m<sup>-3</sup>)</b> |
|---------------------------|-----------------------------------|-----------------------------------|
| <b>B<sub>b</sub></b>      | 15.1                              | 3.02                              |
| <b>B<sub>f</sub></b>      | 15.1                              | 3.02                              |
| <b>B<sub>myc</sub></b>    | 160                               | 32                                |
| <b>B<sub>bvores</sub></b> | 0.1                               | 0.02                              |
| <b>B<sub>fvores</sub></b> | 0.8                               | 0.16                              |
| <b>B<sub>det</sub></b>    | 0.6                               | 0.12                              |
| <b>B<sub>eng</sub></b>    | 0.2                               | 0.04                              |
| <b>B<sub>hvores</sub></b> | 0.2                               | 0.04                              |
| <b>B<sub>pred</sub></b>   | 0.4                               | 0.04                              |
| <b>Litter</b>             | 2680                              | 335                               |
| <b>SOM</b>                | 11470                             | 1433.75                           |

1

**Table 3**(on next page)

Lower and upper bounds for the  $g_{\max}$  prior probability distribution, for each one of the nine functional groups in the food web.

| <b>gmax</b>         | <b>Lower bounds</b> | <b>Upper bounds</b> |
|---------------------|---------------------|---------------------|
| <b>Bacteria</b>     | 1                   | 3                   |
| <b>Fungi</b>        | 0                   | 3                   |
| <b>Mycorrhiza</b>   | 1                   | 3                   |
| <b>Bacterivores</b> | 0                   | 2                   |
| <b>Fungivores</b>   | 0                   | 2                   |
| <b>Detritivores</b> | 0                   | 0.5                 |
| <b>Engineers</b>    | 0                   | 0.5                 |
| <b>Herbivores</b>   | 0                   | 0.5                 |
| <b>Predators</b>    | 0                   | 0.5                 |

1

**Table 4**(on next page)

Averages  $\pm$  standard deviation from the sample of 100  $g_{\max}$  vectors from the posterior distribution of the KEYLINK model calibrated for the Brasschaat Scots pine forest.

| Sample $g_{\max}$   |                   |
|---------------------|-------------------|
| <b>Bacteria</b>     | $1.970 \pm 0.424$ |
| <b>Fungi</b>        | $0.295 \pm 0.134$ |
| <b>Mycorrhiza</b>   | $2.208 \pm 0.302$ |
| <b>Bacterivores</b> | $0.205 \pm 0.098$ |
| <b>Fungivores</b>   | $0.095 \pm 0.050$ |
| <b>Detritivores</b> | $0.091 \pm 0.050$ |
| <b>Engineers</b>    | $0.292 \pm 0.062$ |
| <b>Herbivores</b>   | $0.028 \pm 0.018$ |
| <b>Predators</b>    | $0.408 \pm 0.060$ |

1

**Table 5** (on next page)

Effect of changes in input parameters on the average C pool (in  $\text{g C m}^{-3}$ ) size over 10 years.

Averages from 100 runs of ten years with  $g_{\text{max}}$  parameter sets of the sample from the posterior distribution. The "basal" column has the results using reference input parameters (**Supplemental File S2**), and the other columns show the results with lower litter recalcitrance (rec 20%), lower input litter C:N ratio ( $\text{C:N}_{\text{lit}}$  40), higher pH (5.9), excluding predators ( $B_{\text{pred}}$  0) and a higher clay content in the soil (clay 15%), respectively.

| <b>C pools</b>                            | <b>basal</b> | <b>rec 20%</b> | <b>CN<sub>lit</sub> 40</b> | <b>pH 5.9</b> | <b>B<sub>pred</sub> 0</b> | <b>clay 15%</b> |
|---|--------------|----------------|----------------------------|---------------|---------------------------|-----------------|
| <b>Bacteria</b> (g C/m <sup>3</sup> )     | 5,98         | 6,94           | 6,35                       | 5,90          | 2,67                      | 4,75            |
| <b>Fungi</b> (g C/m <sup>3</sup> )        | 210,14       | 224,83         | 231,33                     | 158,06        | 30,70                     | 141,83          |
| <b>Mycorrhiza</b> (g C/m <sup>3</sup> )   | 39,83        | 40,20          | 40,03                      | 38,70         | 29,75                     | 39,27           |
| <b>Bacterivores</b> (g C/m <sup>3</sup> ) | 0,00         | 0,00           | 0,00                       | 0,00          | 0,03                      | 0,00            |
| <b>Fungivores</b> (g C/m <sup>3</sup> )   | 0,30         | 0,31           | 0,39                       | 0,18          | 0,90                      | 0,40            |
| <b>Detritivores</b> (g C/m <sup>3</sup> ) | 2,49         | 2,12           | 2,01                       | 3,83          | 145,39                    | 0,87            |
| <b>Engineers</b> (g C/m <sup>3</sup> )    | 0,04         | 0,04           | 0,04                       | 0,51          | 1,54                      | 0,05            |
| <b>Herbivores</b> (g C/m <sup>3</sup> )   | 0,12         | 0,12           | 0,13                       | 0,02          | 5,48                      | 0,16            |
| <b>Predators</b> (g C/m <sup>3</sup> )    | 3,33         | 2,86           | 2,87                       | 6,41          | 0,00                      | 1,36            |
| <b>Litter</b> (g C/m <sup>3</sup> )       | 3695,08      | 3262,71        | 3481,79                    | 3728,85       | 2727,81                   | 4245,54         |
| <b>SOM</b> (g C/m <sup>3</sup> )          | 10825,04     | 10941,01       | 10742,97                   | 9347,23       | 3175,08                   | 11655,70        |

1

2

3

**Table 6** (on next page)

Effect of changes in input parameters on the posterior distribution of C pool (in g C m<sup>-3</sup>) size over 10 years.

Minimum and maximum values within 100 runs of ten years with  $g_{\max}$  parameter sets of the sample from the posterior distribution. The "basal" columns have the results using reference input parameters (**Supplemental File S2**), and the following columns show the same changes from basal as in **Table 5**. For C pool notation see **Table 2**.

| <b>C pools</b>                                | <b>basal</b> |         | <b>rec 20%</b> |         | <b>CN<sub>lit</sub> 40</b> |         | <b>pH 5.9</b> |         | <b>B<sub>pred</sub> 0</b> |         | <b>clay 15%</b> |         |
|---|--------------|---------|----------------|---------|----------------------------|---------|---------------|---------|---------------------------|---------|-----------------|---------|
|   | min          | max     | min            | max     | min                        | max     | min           | max     | min                       | max     | min             | max     |
| <b>B<sub>b</sub></b><br>(g C/m <sup>3</sup> ) | 9,61E-42     | 670,64  | 3,41E-43       | 676,40  | 8,48E-38                   | 683,87  | 0,00          | 669,74  | 0,00                      | 547,97  | 8,06E-43        | 788,31  |
| <b>B<sub>f</sub></b>                          | 2,63E-25     | 4660,93 | 3,87E-25       | 4587,16 | 3,74E-25                   | 4677,78 | 0,00          | 4656,39 | 0,00                      | 4038,09 | 2,56E-25        | 4763,21 |
| <b>B<sub>myc</sub></b>                        | 4,18         | 649,45  | 5,11           | 684,88  | 5,79                       | 652,73  | 0,00          | 648,45  | 0,00                      | 592,13  | 5,87            | 515,60  |
| <b>B<sub>bvores</sub></b>                     | 6,89E-110    | 0,10    | 4,91E-105      | 0,10    | 1,17E-108                  | 0,10    | 0,00          | 0,10    | 0,00                      | 44,07   | 1,13E-96        | 0,10    |
| <b>B<sub>fvores</sub></b>                     | 4,47E-84     | 194,08  | 5,82E-84       | 169,06  | 5,28E-83                   | 204,50  | 0,00          | 141,68  | 0,00                      | 351,94  | 1,27E-74        | 244,39  |
| <b>B<sub>det</sub></b>                        | 1,13E-67     | 1720,93 | 3,76E-67       | 1524,58 | 3,02E-68                   | 1567,73 | 0,00          | 6898,50 | 0,00                      | 5997,90 | 7,56E-79        | 431,85  |
| <b>B<sub>eng</sub></b>                        | 7,13E-178    | 61,50   | 6,54E-176      | 33,87   | 5,45E-172                  | 74,46   | 0,00          | 396,62  | 0,00                      | 88,62   | 7,18E-140       | 43,86   |
| <b>B<sub>hvores</sub></b>                     | 1,11E-68     | 49,65   | 5,23E-65       | 49,75   | 1,78E-65                   | 49,64   | 3,78E-89      | 34,32   | 7,95E-22                  | 85,00   | 1,12E-56        | 51,33   |
| <b>B<sub>pred</sub></b>                       | 4,72E-21     | 1616,28 | 4,73E-21       | 1409,80 | 4,72E-21                   | 1466,09 | 0,00          | 5512,93 | 0,00                      | 0,28    | 4,60E-21        | 452,07  |
| <b>Litter</b>                                 | 6,0E+01      | 9056,63 | 42,89          | 8850,72 | 53,95                      | 8996,91 | 60,08         | 8749,61 | 63,63                     | 7409,28 | 75,00           | 9257,38 |
| <b>SOM</b>                                    | 2,35E+3      | 15687,9 | 2356,64        | 16027,4 | 2350,89                    | 15751,5 | 921,46        | 15687,4 | 1340,6                    | 11589,  | 3919,25         | 15842,3 |

|  |  |   |  |   |  |   |  |   |  |   |  |   |  |   |
|--|--|---|--|---|--|---|--|---|--|---|--|---|--|---|
|  |  | 7 |  | 9 |  | 6 |  | 4 |  | 6 |  | 4 |  | 9 |
|--|--|---|--|---|--|---|--|---|--|---|--|---|--|---|

1

**Table 7** (on next page)

Effect of changes in input parameter on major output fluxes over 10 years.

The first three rows show bacterial, fungal and mycorrhiza respiration (R) fluxes ( $\text{g C m}^{-3}$ ), respectively. The next three rows show the total turnover ( $\text{g C m}^{-3}$ ) on an organic matter pool carried out by bacteria (Bact) or engineers (Eng) over 10 years. The penultimate row shows the fungi to bacteria ratio. And the last row is soil water content (SWC,  $\text{l m}^{-3}$ ). Columns show average values and standard deviations from 100 runs of ten years from the sample of the posterior distribution, with a basal scenario using reference input parameters (**Supplemental File S2**), and the same changes from it as in **Table 5**.

|   | units               | basal         | rec 20%       | C:N <sub>lit</sub> 40 | pH 5.9        | B <sub>pred</sub> 0 | clay 15%      |
|---|---------------------|---------------|---------------|-----------------------|---------------|---------------------|---------------|
| <b>R<sub>bact</sub></b>                   | g C m <sup>-3</sup> | 250.2±222.8   | 293.6±227.2   | 262.3±225.7           | 248.9±222.4   | 119.3±149.9         | 204.5±225.9   |
| <b>R<sub>fun</sub></b>                    | g C m <sup>-3</sup> | 3924.8±5043.6 | 4190.0±5035.6 | 4215.4±5166.1         | 3400.6±4776.3 | 963.6±2669.4        | 2638.5±4270.7 |
| <b>R<sub>myc</sub></b>                    | g C m <sup>-3</sup> | 773.9±443.7   | 785.3±447.3   | 779.1±445.9           | 760.4±431.3   | 560.3±335.5         | 760.5±447.5   |
| <b>Bact SOM turnover</b>                  | g C m <sup>-3</sup> | 995.6±758.2   | 1100.2±716.3  | 1036.5±757.7          | 985.4±752.6   | 438.6±524.2         | 780.2±741.7   |
| <b>Bact litter turnover</b>               | g C m <sup>-3</sup> | 258.6±264.1   | 367.7±328.6   | 280.2±276.2           | 257.6±263.9   | 119.6±170.6         | 223.5±279.7   |
| <b>Eng litter turnover</b>                | g C m <sup>-3</sup> | 1.5±5.3       | 1.3±4.5       | 1.3±4.4               | 43.8±104.4    | 97.3±72.1           | 2.0±5.8       |
| <b>B<sub>fungi</sub>/B<sub>bact</sub></b> | -                   | 35.2          | 32.4          | 36.4                  | 26.8          | 11.5                | 29.9          |
| <b>SWC</b>                                | l m <sup>-3</sup>   | 147.9±32.7    | 149.2±32.4    | 150.3±33.7            | 144.2±31.1    | 134.2±21.8          | 321.6±27.2    |

1

# Figure 1

Simplified model scheme.

General structure of the KEYLINK model. Square boxes represent pools of organic matter. Wide double-line arrows, with a circle within the arrow, represent fluxes between pools (blue arrowheads show bidirectional fluxes). Isolated circles represent abiotic factors that affect model fluxes, and red narrow arrows connect each factor or pool with the model parts (at the arrowheads) that are regulated by them.

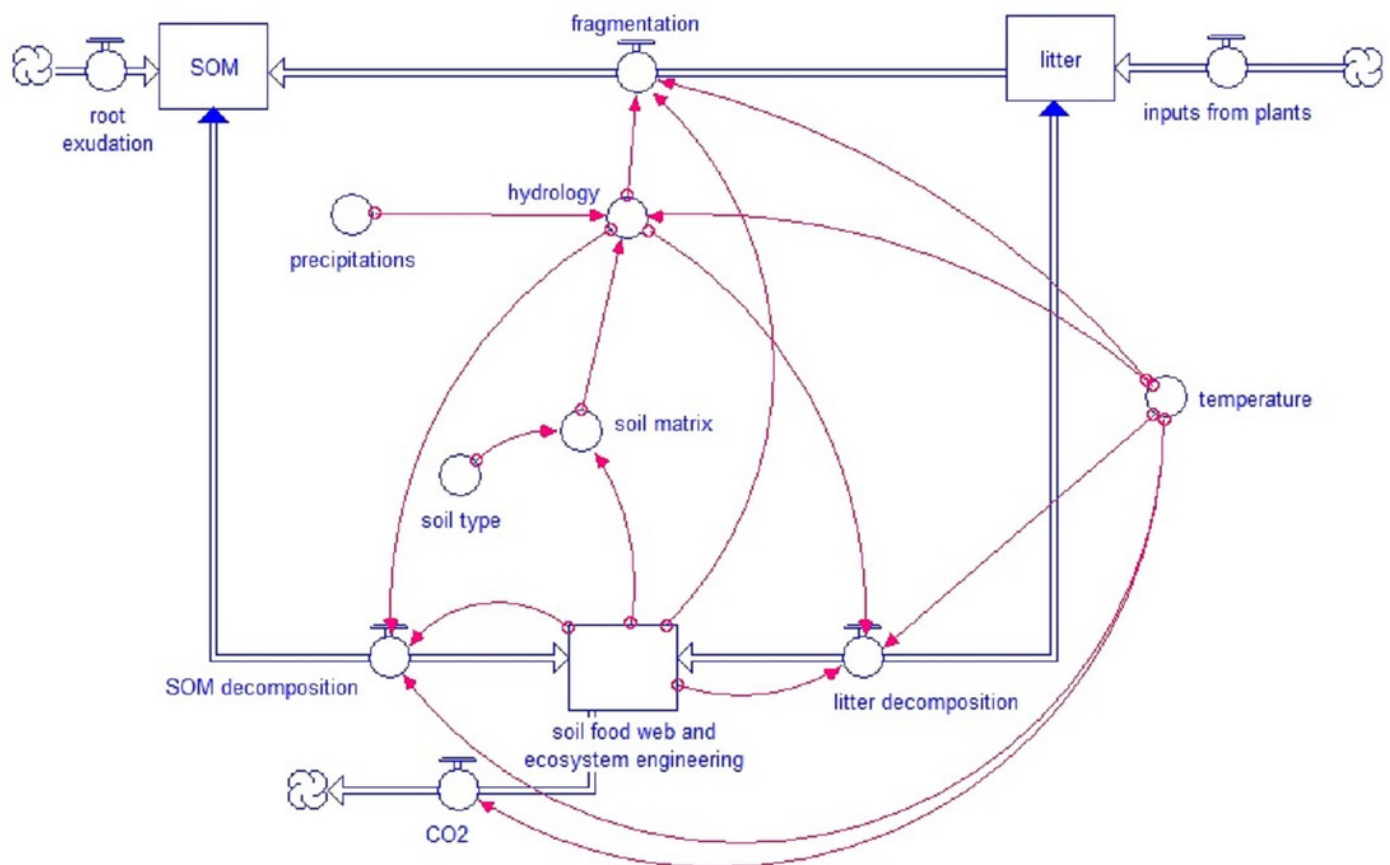


## Figure 2

Pools and fluxes in the KEYLINK model.

Scheme of C pools with their interactions. All pools, soil, microorganisms and fauna (see **Table S1.2 in Supplemental File S1**) are represented in the model in the same units ( $\text{g C m}^{-3}$ ). The arrows represent carbon fluxes between the pools; each arrow is represented by a term in the model equations.

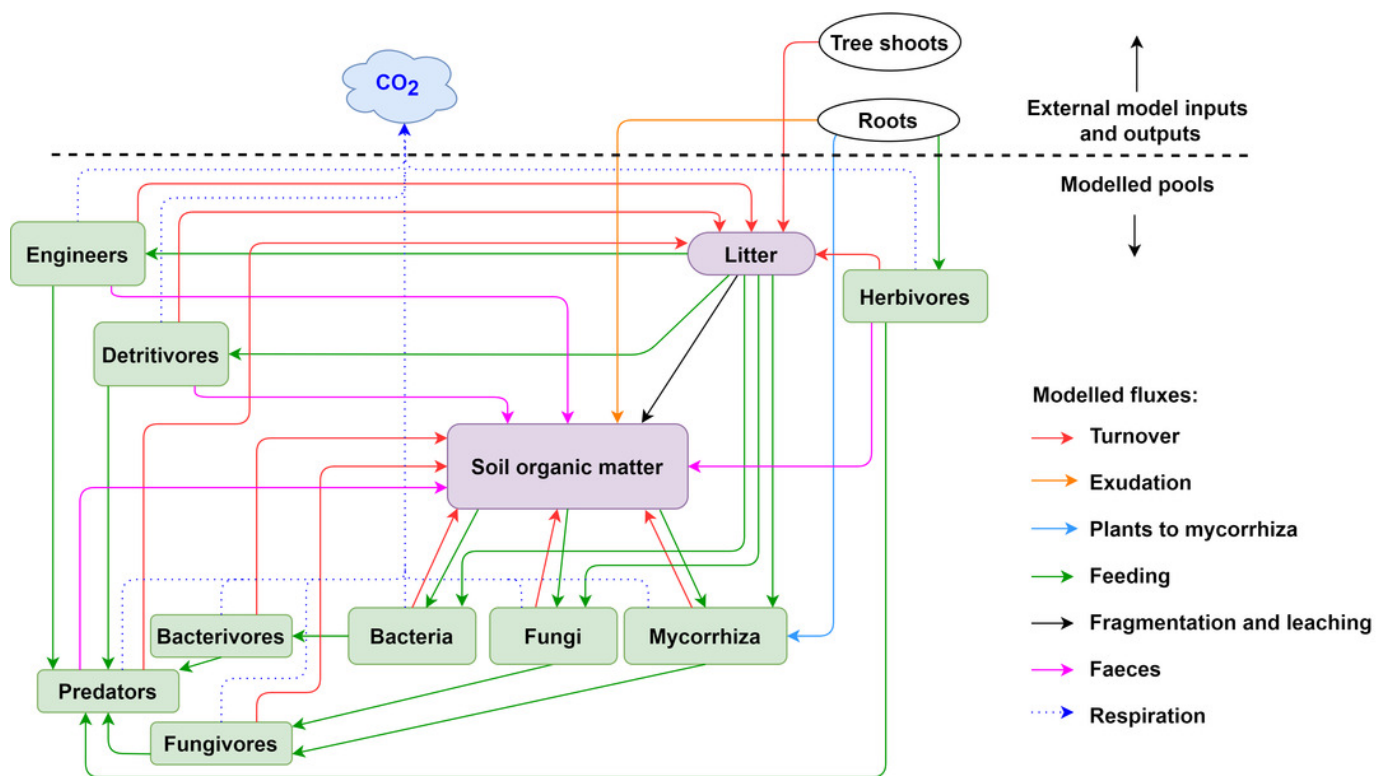


## Figure 3

C pools daily biomass averages and standard deviations from the basal scenario

C pools (in  $\text{g C m}^{-3}$ ) averages (black) and standard deviations (grey) among 100 simulations of ten years using the  $g_{\max}$  sample from the basal simulation scenario. **A)** bacteria pool; **B)** non-mycorrhizal fungi; **C)** mycorrhizal fungi; **D)** microbivores feeding on bacteria; **E)** microbivores feeding on fungi; **F)** non-engineer detritivores; **G)** ecosystem engineers; **H)** herbivores; **I)** predators; **J)** plant litter; **K)** soil organic matter.

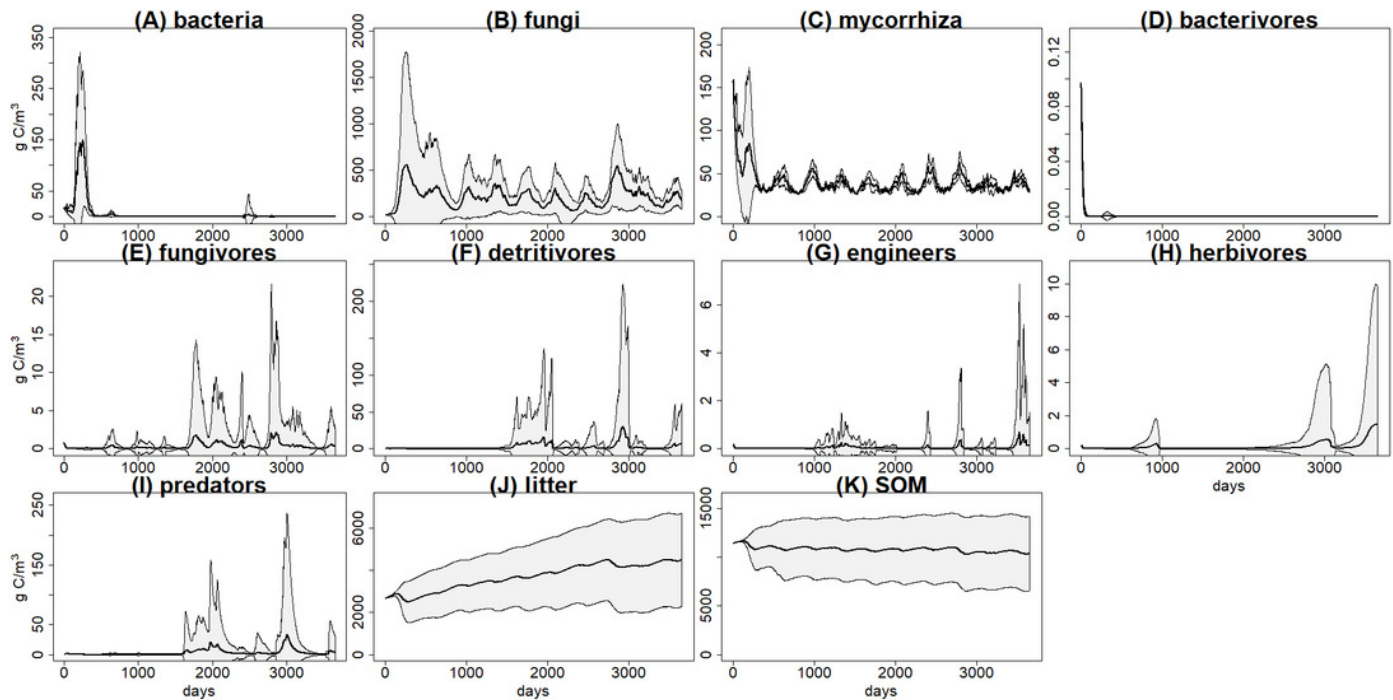


## Figure 4

C pools daily biomass averages under different scenarios.

Averages of C pools (in  $\text{g C m}^{-3}$ ) among 100 simulations of ten years using the  $g_{\text{max}}$  sample, with the basal simulation (black solid lines), and the alternative scenarios: higher clay content (red dashed lines), lower input litter C:N (yellow dotted lines), excluding predators (dark blue dotted dashed lines), higher soil pH (green long dash lines) and lower litter recalcitrance (light blue, lines with two different dashes). Pools are the same as in **Figure 3**, i.e. the nine food web functional groups, litter and soil organic matter (SOM).

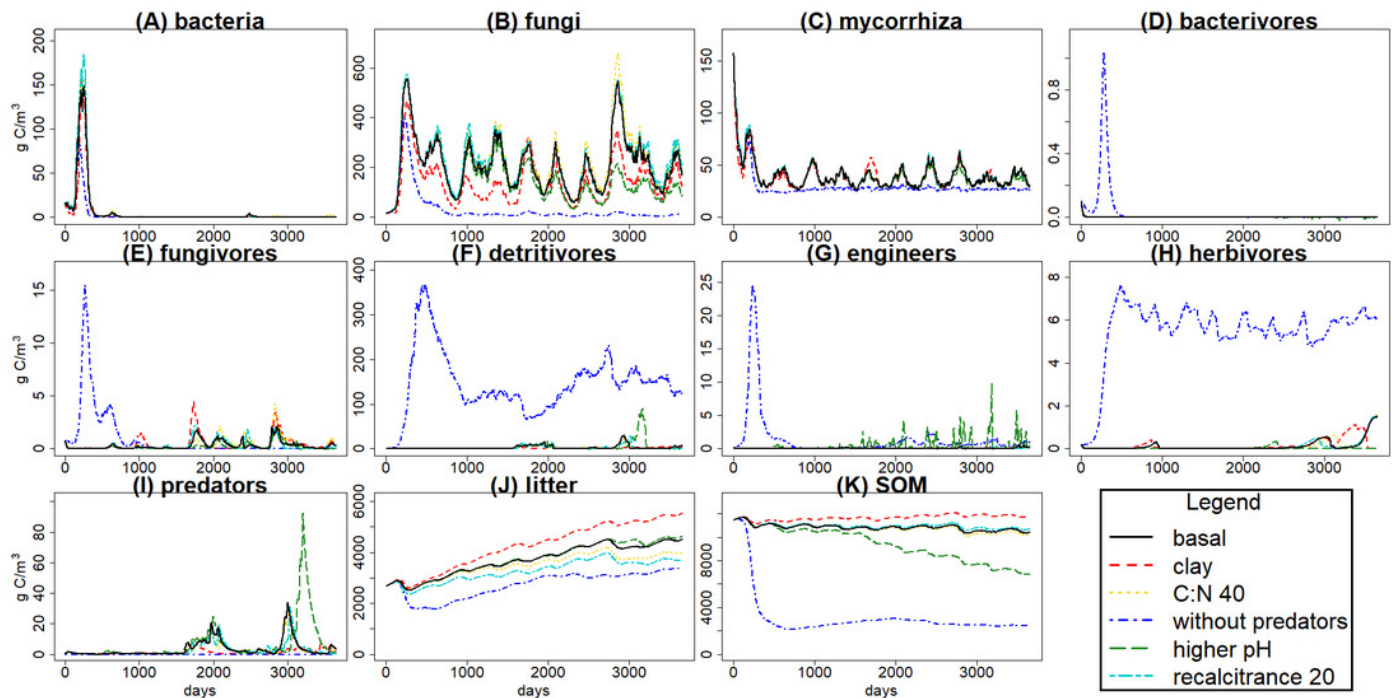


## Figure 5

Daily volume averages of soil water content (SWC) and pore size classes in the soil matrix.

Means of volume (in  $l\ m^{-3}$ ) among 100 simulations of ten years using the sample of  $g_{max}$  vectors, for the evaluation scenarios (see **Figure 4**). Graphs **A-D** for pore size classes, **E** for SWC. The inaccessible pore size class is not shown because it was not affected by changes in porosity.

